

1 **Mitochondrial respiratory states and rates:**
2 **Building blocks of mitochondrial physiology**
3 **Part 1.** MitoEAGLE preprint 2018-02-25(30)
4

5 http://www.mitoeagle.org/index.php/MitoEAGLE_preprint_2018-02-08
6

7 Preprint version 30 (2018-02-25)

8 **MitoEAGLE Network**

9 Corresponding author: Gnaiger E

10 Contributing co-authors

11 Aasander Frostner E, Acuna-Castroviejo D, Ahn B, Alves MG, Amati F, Aral C,
12 Arandarčikaitė O, Bailey DM, Bakker BM, Bastos Sant'Anna Silva AC, Battino M, Beard
13 DA, Ben-Shachar D, Bishop D, Borutaitė V, Breton S, Brown GC, Brown RA, Buettner GR,
14 Burtscher J, Calabria E, Calbet JA, Cardoso LHD, Carvalho E, Casado Pinna M, Cervinkova
15 Z, Chang SC, Chaurasia B, Chen Q, Chicco AJ, Chinopoulos C, Clementi E, Coen PM, Collin
16 A, Crisóstomo L, Das AM, Davis MS, De Palma C, Dias TR, Distefano G, Doerrier C,
17 Drahotka Z, Duchon MR, Ehinger J, Elmer E, Endlicher R, Fell DA, Ferko M, Ferreira JCB,
18 Filipovska A, Fisar Z, Fischer M, Fisher JJ, Fornaro M, Galkin A, Garcia-Roves PM, Garcia-
19 Souza LF, Genova ML, Giovarelli M, Gonzalez-Arment JL, Gonzalo H, Goodpaster BH,
20 Gorr TA, Gourlay CW, Granata C, Grefte S, Haas CB, Haavik J, Han J, Harrison DK,
21 Hellgren KT, Hernansanz-Agustin P, Holland O, Hoppel CL, Houstek J, Hunger M, Iglesias-
22 Gonzalez J, Irving BA, Iyer S, Jackson CB, Jadiya P, Jang DH, Jansen-Dürr P, Jespersen NR,
23 Jha RK, Kaambre T, Kane DA, Kappler L, Karabatsiakos A, Keijer J, Keppner G,
24 Klingenspor M, Komlodi T, Koopman WJH, Kopitar-Jerala N, Krako Jakovljevic N, Kuang J,
25 Kucera O, Labieniec-Watala M, Lai N, Laner V, Larsen TS, Lee HK, Lemieux H, Lerfall J,
26 Liu J, Lucchinetti E, MacMillan-Crow LA, Makrečka-Kuka M, Malik A, Markova M,
27 Meszaros AT, Michalak S, Moiso N, Molina AJA, Montaigne D, Moore AL, Moreira BP,
28 Mracek T, Muntane J, Muntean DM, Murray AJ, Nemeč M, Neuzil J, Newsom S, Nozickova
29 K, O'Gorman D, Oliveira MT, Oliveira PF, Oliveira PJ, Orynbayeva Z, Pak YK, Palmeira
30 CM, Patel HH, Pecina P, Pelena D, Pereira da Silva Grilo da Silva F, Pesta D, Petit PX,
31 Pichaud N, Piel S, Pirkmajer S, Porter RK, Pranger F, Prochownik EV, Pulini Kunnil T,
32 Puurand M, Radenkovic F, Radi R, Ramzan R, Reboredo P, Renner-Sattler K, Robinson MM,
33 Rohlena J, Ropelle ER, Røslund GV, Rossiter HB, Rybacka-Mossakowska J, Saada A, Safaei
34 Z, Salvadego D, Sandi C, Scatena R, Schartner M, Scheibye-Knudsen M, Schilling JM,
35 Schlattner U, Schönfeld P, Schwarzer C, Scott GR, Shabalina IG, Sharma P, Sharma V,
36 Shevchuk I, Siewiera K, Silber AM, Singer D, Smenes BT, Soares FAA, Sobotka O,
37 Sokolova I, Spinazzi M, Stankova P, Stier A, Stocker R, Sumbalova Z, Suravajhala P,
38 Swerdlow RH, Swiniuch D, Tanaka M, Tandler B, Tepp K, Tomar D, Towheed A, Tretter L,
39 Trifunovic A, Trivigno C, Tronstad KJ, Trougakos IP, Tyrrell DJ, Urban T, Valentine JM,
40 Velika B, Vendelin M, Vercesi AE, Victor VM, Villena JA, Vogt S, Volani C, Votion DM,
41 Vujacic-Mirski K, Wagner BA, Ward ML, Watala C, Wei YH, Wieckowski MR, Williams C,
42 Wohlwend M, Wolff J, Wuest RCI, Zaugg K, Zaugg M, Zischka H, Zorzano A

43 Supporting co-authors:

44 Bernardi P, Boetker HE, Borsheim E, Bouitbir J, Calzia E, Coker RH, Dubouchaud H,
45 Durham WJ, Dyrstad SE, Engin AB, Gan Z, Garlid KD, Garten A, Haendeler J, Hand SC,
46 Hepple RT, Hickey AJ, Hoel F, Kainulainen H, Khamoui AV, Kowaltowski AJ, Krajcova A,
47 Lane N, Lenaz G, Liu SS, Mazat JP, Menze MA, Methner A, Nedergaard J, Pallotta ML,
48 Parajuli N, Pettersen IK, Porter C, Salin K, Sazanov LA, Skolik R, Sonkar VK, Szabo I,
49 Thyfault JP, Vieyra A
50
51

Updates and discussion:

http://www.mitoeagle.org/index.php/MitoEAGLE_preprint_2018-02-08

Correspondence: Gnaiger E

Chair COST Action CA15203 MitoEAGLE – <http://www.mitoeagle.org>

Department of Visceral, Transplant and Thoracic Surgery, D. Swarovski Research
Laboratory, Medical University of Innsbruck, Innrain 66/4, A-6020 Innsbruck, Austria

Email: mitoeagle@i-med.ac.at

Tel: +43 512 566796, Fax: +43 512 566796 20

Contents**Abstract****Executive summary****1. Introduction** – Box 1: In brief: Mitochondria and Bioblasts**2. Oxidative phosphorylation and coupling states in mitochondrial preparations**

Mitochondrial preparations

2.1. Respiratory control and coupling

The steady-state

Specification of biochemical dose

Phosphorylation, P_{\gg} , and P_{\gg}/O_2 ratio

Control and regulation

Respiratory control and response

Respiratory coupling control and ET-pathway control

Coupling

Uncoupling

2.2. Coupling states and respiratory rates

Respiratory capacities in coupling control states

LEAK, OXPHOS, ET, ROX

2.3. Classical terminology for isolated mitochondria

States 1–5

3. Normalization: fluxes and flows*3.1. Normalization: system or sample*

Flow per system, I

Extensive quantities

Size-specific quantities – Box 2: Metabolic fluxes and flows: vectorial and scalar

3.2. Normalization for system-size: flux per chamber volume

System-specific flux, J_{V,O_2}

3.3. Normalization: per sample

Sample concentration, C_{mX}

Mass-specific flux, $J_{O_2/mX}$

Number concentration, C_{NX}

Flow per object, $I_{O_2/X}$

3.4. Normalization for mitochondrial content

Mitochondrial concentration, C_{mtE} , and mitochondrial markers

Mitochondria-specific flux, $J_{O_2/mtE}$

*3.5. Evaluation of mitochondrial markers**3.6. Conversion: units***4. Conclusions** – Box 3: Mitochondrial and cell respiration**5. References**

102 **Abstract** As the knowledge base and importance of mitochondrial physiology to human health
 103 expands, the necessity for harmonizing nomenclature concerning mitochondrial respiratory
 104 states and rates has become increasingly apparent. Clarity of concept and consistency of
 105 nomenclature are key trademarks of a research field. These trademarks facilitate effective
 106 transdisciplinary communication, education, and ultimately further discovery. The
 107 chemiosmotic theory establishes the mechanism of energy transformation and coupling in
 108 oxidative phosphorylation. The unifying concept of the protonmotive force provides the
 109 framework for developing a consistent theoretical foundation of mitochondrial physiology and
 110 bioenergetics. We follow IUPAC guidelines on terminology in physical chemistry, extended
 111 by considerations on open systems and irreversible thermodynamics. The concept-driven
 112 constructive terminology incorporates the meaning of each quantity and aligns concepts and
 113 symbols to the nomenclature of classical bioenergetics. In the frame of COST Action
 114 MitoEAGLE open to global bottom-up input, we endeavour to provide a balanced view on
 115 mitochondrial respiratory control and a critical discussion on reporting data of mitochondrial
 116 respiration in terms of metabolic flows and fluxes. Uniform standards for evaluation of
 117 respiratory states and rates will ultimately support the development of databases of
 118 mitochondrial respiratory function in species, tissues, and cells.

119

120 *Keywords:* Mitochondrial respiratory control, coupling control, mitochondrial
 121 preparations, protonmotive force, uncoupling, oxidative phosphorylation, OXPHOS,
 122 efficiency, electron transfer, ET; proton leak, LEAK, residual oxygen consumption, ROX, State
 123 2, State 3, State 4, normalization, flow, flux, O₂

124

125

126

127

127 **Executive summary**

128

129

130

131

132

133

134

135

136

137

138

139

140

141

142

143

144

145

146

147

148

149

150

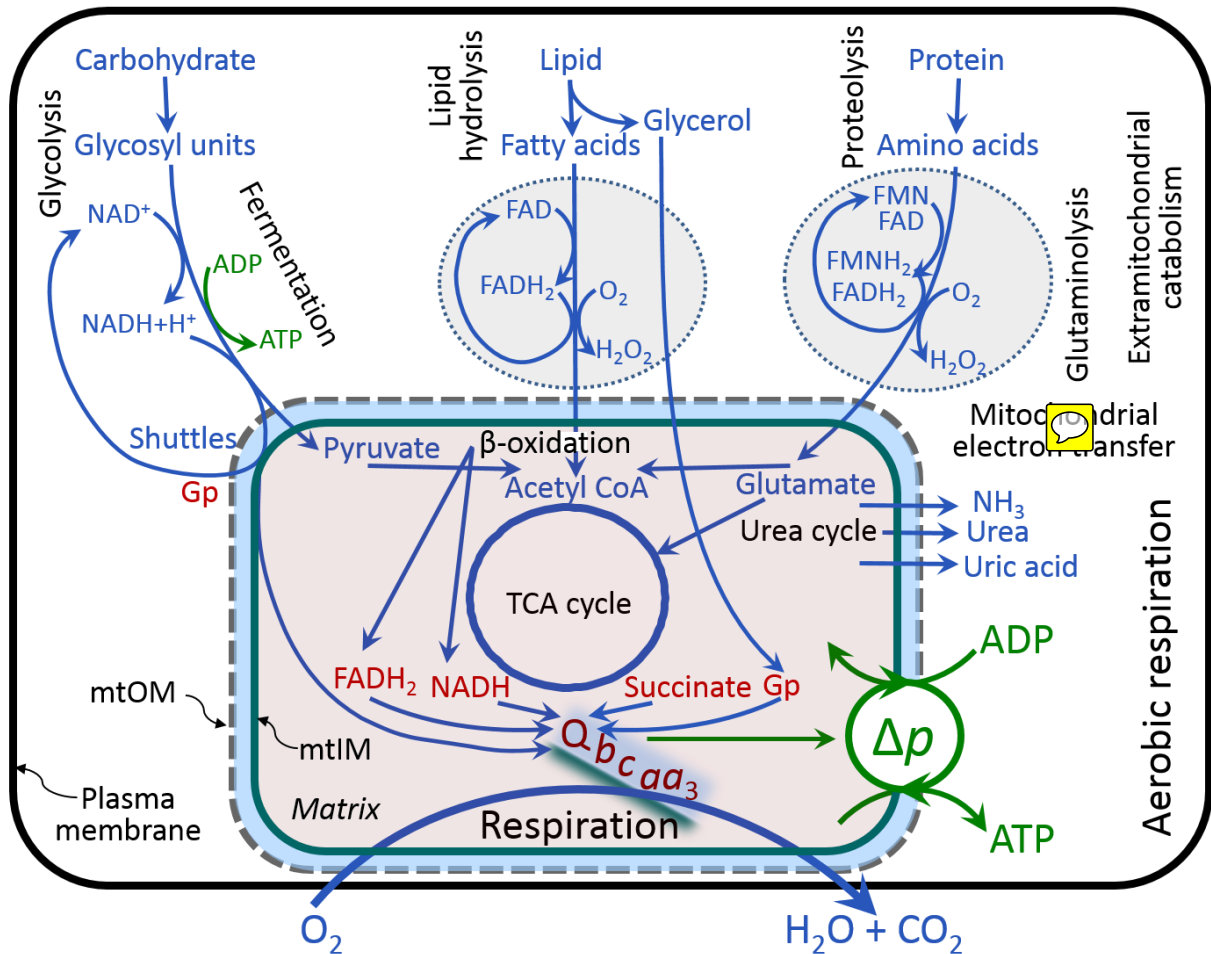
151

152

1. In view of broad implications on health care, mitochondrial researchers face an increasing responsibility to disseminate their fundamental knowledge and novel discoveries to a wide range of stakeholders and scientists beyond the group of specialists. This requires implementation of a commonly accepted terminology within the discipline and standardization in the translational context. Authors, reviewers, journal editors, and lecturers are challenged to collaborate with the aim to harmonize the nomenclature in the growing field of mitochondrial physiology and bioenergetics.
2. Aerobic energy metabolism in mitochondria of most eukaryotic cells depends on the coupling of phosphorylation (ADP → ATP) to O₂ flux in catabolic reactions. In this process of oxidative phosphorylation, coupling is mediated by translocation of protons through respiratory proton pumps operating across the inner mitochondrial membrane and generating or utilizing the protonmotive force measured between the mitochondrial matrix and intermembrane compartment. Compartmental coupling thus distinguishes vectorial oxidative phosphorylation from fermentation as the counterpart of cellular core energy metabolism (**Fig. 1**).
3. To exclude fermentation and other cytosolic interactions from exerting an effect on mitochondrial metabolism, the barrier function of the plasma membrane must be disrupted. Selective removal or permeabilization of the plasma membrane yields mitochondrial preparations—including isolated mitochondria, tissue and cellular preparations—with structural and functional integrity. Then extra-mitochondrial concentrations of fuel substrates transported into the mitochondrial matrix, ADP, ATP, inorganic phosphate, and cations including H⁺ can be controlled to determine mitochondrial function under a set of conditions defined as coupling control states.

153
154
155
156

A concept-driven terminology of bioenergetics incorporates in its terms and symbols explicit information on the nature of respiratory states, that makes the technical terms readily recognized and easy to understand.



157
158
159
160
161
162
163
164
165
166
167
168
169
170
171
172
173
174
175
176
177

Fig. 1. Respiration in the framework of cellular catabolic energy metabolism. Aerobic respiration is the utilization of the products of extramitochondrial catabolism for electron transfer to O₂ as the electron acceptor. In catabolic energy transformation, catabolic reactions are coupled to the phosphorylation of ADP to ATP, mediated by the protonmotive force, Δp . Glycolysis involves substrate-level phosphorylation of ADP to ATP in anaerobic fermentation. In contrast, partial extramitochondrial oxidation of fatty acids and amino acids proceeds in peroxisomes (dotted spheres) without coupling to ATP production: acyl-CoA oxidase catalyzes the oxidation of FADH₂ with electron transfer to O₂; amino acid oxidases oxidize FMNH₂ or FADH₂. Mitochondrial outer and inner membrane, mtOM and mtIM. Coenzyme Q, Q, and the cytochromes *b*, *c*, and *aa*₃ are redox systems of the mtIM. Glycerol-3-phosphate, Gp; tricarboxylic acid cycle, TCA cycle.

- Mitochondrial coupling states are defined according to the control of respiratory oxygen flux by the protonmotive force. Capacities of oxidative phosphorylation and electron transfer capacities are measured at kinetically saturating concentrations of fuel substrates, ADP and inorganic phosphate, or at optimal uncoupler concentrations, respectively. Respiratory capacities are a measure of the upper bound of the rates of respiration, providing reference values for the diagnosis of health and disease, and for evaluation of the effects of Evolutionary background, Age, Gender and sex, Lifestyle and Environment (EAGLE).

- 178 5. Some degree of uncoupling is a characteristic of energy-transformations across
179 membranes. Uncoupling is caused by a variety of physiological, pathological,
180 toxicological, pharmacological and environmental conditions that exert an
181 influence not only on the proton leak and cation cycling, but also on proton slip
182 within the proton pumps and the structural integrity of the mitochondria. A more
183 loosely coupled state is induced by stimulation of mitochondrial superoxide
184 formation and the bypass of proton pumps. In addition, uncoupling by application
185 of protonophores represents an experimental intervention for the transition from a
186 well-coupled to the noncoupled state of mitochondrial respiration.
- 187 6. Respiratory oxygen consumption rates have to be carefully normalized to enable meta-
188 analytic studies beyond the specific question of a particular experiment. Therefore,
189 all raw data should be published in a supplemental table or open access data
190 repository. Normalization of rates for the volume of the experimental chamber (the
191 measuring system) is distinguished from normalization for (1) the volume or mass
192 of the experimental sample, (2) the number of objects (cells, organisms), and (3)
193 the concentration of mitochondrial markers in the chamber.
- 194 7. The consistent use of terms and symbols discussed in this MitoEAGLE position
195 statement will facilitate transdisciplinary communication and support further
196 development of a database on bioenergetics and mitochondrial physiology. The
197 present considerations are focused on studies with mitochondrial preparations.
198 These will be extended in a series of reports on pathway control of mitochondrial
199 respiration, the protonmotive force, respiratory states in intact cells, and
200 harmonization of experimental procedures.
201
-
- 202
203
-

204 **Box 1: In brief – Mitochondria and Bioblasts**

205 **Mitochondria** are the oxygen-consuming electrochemical generators evolved from
206 endosymbiotic bacteria (Margulis 1970; Lane 2005). They were described by Richard Altmann
207 (1894) as ‘bioblasts’, which include not only the mitochondria as presently defined, but also
208 symbiotic and free-living bacteria. The word ‘mitochondria’ (Greek mitos: thread; chondros:
209 granule) was introduced by Carl Benda (1898).

210 Mitochondria are dynamic networks contained within eukaryotic cells morphologically
211 characterized by a double membrane. The mitochondrial inner membrane (mtIM) shows
212 dynamic tubular to disk-shaped cristae that separate the mitochondrial matrix, *i.e.*, the
213 negatively charged internal mitochondrial compartment, from the intermembrane space; the
214 latter being positively charged and enclosed by the mitochondrial outer membrane (mtOM).
215 The mtIM contains the non-bilayer phospholipid cardiolipin, which is not present in any other
216 eukaryotic cellular membrane. Cardiolipin promotes the formation of respiratory
217 supercomplexes (SC I_nIII_nIV_n), which are supramolecular assemblies based upon specific,
218 though dynamic interactions between individual respiratory complexes (Greggio *et al.* 2017;
219 Lenaz *et al.* 2017). Membrane fluidity exerts an influence on functional properties of proteins
220 incorporated in the membranes (Waczulikova *et al.* 2007).
221

222 Mitochondria are the structural and functional elements of cell respiration. Cell
223 respiration is the reduction of oxygen by electron transfer coupled to electrochemical proton
224 translocation across the mtIM. In the process of oxidative phosphorylation (OXPHOS), the
225 catabolic reaction of oxygen consumption is electrochemically coupled to the transformation of
226 energy in the form of adenosine triphosphate (ATP; Mitchell 1961, 2011). Mitochondria are the
227 powerhouses of the cell which contain the machinery of the OXPHOS-pathways, including
228

229 transmembrane respiratory complexes—proton pumps with FMN, Fe-S and cytochrome *b*, *c*,
 230 *aa₃* redox systems); alternative dehydrogenases and oxidases; the coenzyme ubiquinone (Q);
 231 F-ATPase or ATP synthase; the enzymes of the tricarboxylic acid cycle, fatty acid and
 232 aminoacid oxidation; transporters of ions, metabolites and co-factors; and mitochondrial
 233 kinases related to energy transfer pathways. The mitochondrial proteome comprises over 1,200
 234 proteins (Calvo *et al.* 2015; 2017), mostly encoded by nuclear DNA (nDNA), with a variety of
 235 functions, many of which are relatively well known (*e.g.*, proteins regulating mitochondrial
 236 biogenesis or apoptosis), while others are still under investigation, or need to be identified (*e.g.*,
 237 alanine transporter).

238 There is a constant crosstalk between mitochondria and the other cellular components.
 239 The crosstalk between mitochondria and endoplasmic reticulum is involved in the regulation of
 240 calcium homeostasis, cell division, autophagy, differentiation, anti-viral signaling (Murley and
 241 Nunnari 2016). Mitochondria contribute to the formation of peroxisomes, which are hybrids of
 242 mitochondrial and ER-derived precursors (Sugiura *et al.* 2017). Cellular mitostasis is
 243 maintained through regulation at both the transcriptional and post-translational level, through
 244 cell signalling including proteostatic (*e.g.*, the ubiquitin-proteasome and autophagy-lysosome
 245 pathways), and genome stability modules throughout the cell cycle or even cell death,
 246 contributing to homeostatic regulation in response to varying energy demands and stress
 247 (Quiros *et al.* 2016). In addition to mitochondrial movement along microtubules, mitochondrial
 248 morphology can change in response to energy requirements of the cell via processes known as
 249 fusion and fission, through which mitochondria communicate within a network, and in response
 250 to intracellular stress factors causing swelling and ultimately permeability transition.

251 Mitochondria typically maintain several copies of their own genome known as
 252 mitochondrial DNA (mtDNA; hundred to thousands per cell; Cummins 1998), which is
 253 maternally inherited. Biparental mitochondrial inheritance is documented in mammals, birds,
 254 fish, reptiles and invertebrate groups, and is even the norm in bivalves (Breton *et al.* 2007;
 255 White *et al.* 2008). mtDNA is compact (16.5 kB in humans) and encodes 13 protein subunits
 256 of the transmembrane respiratory Complexes CI, CIII, CIV and F-ATPase, 22 tRNAs, and two
 257 RNAs. Additional gene content has been suggested to include microRNAs, piRNA,
 258 smithRNAs, repeat associated RNA, and even additional proteins (Duarte *et al.* 2014; Lee *et al.*
 259 *et al.* 2015; Cobb *et al.* 2016). The mitochondrial genome requires nuclear-encoded mitochondrial
 260 targeted proteins for its maintenance and expression (Rackham *et al.* 2012).

261 Abbreviation: mt, as generally used in mtDNA. Mitochondrion is singular and
 262 mitochondria is plural.

263 ‘*For the physiologist, mitochondria afforded the first opportunity for an experimental*
 264 *approach to structure-function relationships, in particular those involved in active transport,*
 265 *vectorial metabolism, and metabolic control mechanisms on a subcellular level’ (Ernster and*
 266 *Schatz 1981).*

268
 269

270 1. Introduction

271

272 Mitochondria are the powerhouses of the cell with numerous physiological, molecular,
 273 and genetic functions (**Box 1**). Every study of mitochondrial health and disease is faced with
 274 Evolution, Age, Gender and sex, Lifestyle, and Environment (EAGLE) as essential background
 275 conditions intrinsic to the individual patient or subject, cohort, species, tissue and to some extent
 276 even cell line. As a large and coordinated group of laboratories and researchers, the mission of
 277 the global MitoEAGLE Network is to generate the necessary scale, type, and quality of
 278 consistent data sets and conditions to address this intrinsic complexity. Harmonization of
 279 experimental protocols and implementation of a quality control and data management system

280 are required to interrelate results gathered across a spectrum of studies and to generate a
281 rigorously monitored database focused on mitochondrial respiratory function. In this way,
282 researchers within the same and across different disciplines will be positioned to compare
283 findings across traditions and generations to an agreed upon set of clearly defined and accepted
284 international standards.

285 Reliability and comparability of quantitative results depend on the accuracy of
286 measurements under strictly-defined conditions. A conceptual framework is required to warrant
287 meaningful interpretation and comparability of experimental outcomes carried out by research
288 groups at different institutes. With an emphasis on quality of research, collected data can be
289 useful far beyond the specific question of a particular experiment. Enabling meta-analytic
290 studies is the most economic way of providing robust answers to biological questions (Cooper
291 *et al.* 2009). Vague or ambiguous jargon can lead to confusion and may relegate valuable
292 signals to wasteful noise. For this reason, measured values must be expressed in standard units
293 for each parameter used to define mitochondrial respiratory function. Harmonization of
294 nomenclature and definition of technical terms are essential to improve the awareness of the
295 intricate meaning of current and past scientific vocabulary, for documentation and integration
296 into databases in general, and quantitative modelling in particular (Beard 2005). The focus on
297 coupling states and fluxes through metabolic pathways of aerobic energy transformation in
298 mitochondrial preparations is a first step in the attempt to generate a conceptually-oriented
299 nomenclature in bioenergetics and mitochondrial physiology. Coupling states of intact cells,
300 the protonmotive force, and respiratory control by fuel substrates and specific inhibitors of
301 respiratory enzymes will be reviewed in subsequent communications.

302
303

304 2. Oxidative phosphorylation and coupling states in mitochondrial preparations

305 *‘Every professional group develops its own technical jargon for talking about matters of*
306 *critical concern ... People who know a word can share that idea with other members of*
307 *their group, and a shared vocabulary is part of the glue that holds people together and*
308 *allows them to create a shared culture’* (Miller 1991).

309

310 **Mitochondrial preparations** are defined as either isolated mitochondria, or tissue and
311 cellular preparations in which the barrier function of the plasma membrane is disrupted. Since
312 this entails the loss of cell viability, mitochondrial preparations are not studied *in vivo*. In
313 contrast to isolated mitochondria and tissue homogenate preparations, mitochondria in
314 permeabilized tissues and cells are *in situ* relative to the plasma membrane. The plasma
315 membrane separates the intracellular compartment including the cytosol, nucleus, and
316 organelles from the environment of the cell. The plasma membrane consists of a lipid bilayer,
317 embedded proteins, and attached organic molecules that collectively control the selective
318 permeability of ions, organic molecules, and particles across the cell boundary. The intact
319 plasma membrane prevents the passage of many water-soluble mitochondrial substrates and
320 inorganic ions—such as succinate, adenosine diphosphate (ADP) and inorganic phosphate (P_i),
321 that must be controlled at kinetically-saturating concentrations for the analysis of respiratory
322 capacities; this limits the scope of investigations into mitochondrial respiratory function in
323 intact cells.

324 The cholesterol content of the plasma membrane is high compared to mitochondrial
325 membranes. Therefore, mild detergents—such as digitonin and saponin—can be applied to
326 selectively permeabilize the plasma membrane by interaction with cholesterol and allow free
327 exchange of organic molecules and inorganic ions between the cytosol and the immediate cell
328 environment, while maintaining the integrity and localization of organelles, cytoskeleton, and
329 the nucleus. Application of optimum concentrations of permeabilization agents (mild detergents
330 or toxins) leads to washout of cytosolic marker enzymes—such as lactate dehydrogenase—and

331 results in the complete loss of cell viability, tested by nuclear staining using membrane-
332 impermeable dyes, while mitochondrial function remains intact. Respiration of isolated
333 mitochondria remains unaltered after the addition of low concentrations of digitonin or saponin.
334 In addition to mechanical cell disruption during homogenization of tissue, permeabilization
335 agents may be applied to ensure permeabilization of all cells. Suspensions of cells
336 permeabilized in the respiration chamber and crude tissue homogenates contain all components
337 of the cell at highly dilute concentrations. All mitochondria are retained in chemically-
338 permeabilized mitochondrial preparations and crude tissue homogenates. In the preparation of
339 isolated mitochondria, the cells or tissues are homogenized, and the mitochondria are separated
340 from other cell fractions and purified by differential centrifugation, entailing the loss of a
341 fraction of the total mitochondrial content. Typical mitochondrial recovery ranges from 30% to
342 80%. Maximization of the purity of isolated mitochondria may compromise not only the
343 mitochondrial yield but also the structural and functional integrity. Therefore, protocols to
344 isolate mitochondria need to be optimized according to each study. The term mitochondrial
345 preparation does not include further fractionation of mitochondrial components, neither
346 submitochondrial particles.

347

348 2.1. Respiratory control and coupling

349

350 Respiratory coupling control states are established in studies of mitochondrial
351 preparations to obtain reference values for various output variables. Physiological conditions *in*
352 *vivo* deviate from these experimentally obtained states. Since kinetically-saturating
353 concentrations, *e.g.*, of ADP or oxygen (O₂; dioxygen), may not apply to physiological
354 intracellular conditions, relevant information is obtained in studies of kinetic responses to
355 variations in [ADP] or [O₂] in the range between kinetically-saturating concentrations and
356 anoxia (Gnaiger 2001).

357 **The steady-state:** Mitochondria represent a thermodynamically open system in non-
358 equilibrium states of biochemical energy transformation. State variables (protonmotive force;
359 redox states) and metabolic *rates* (fluxes) are measured in defined mitochondrial respiratory
360 *states*. Steady-states can be obtained only in open systems, in which changes by *internal*
361 transformations, *e.g.*, O₂ consumption, are instantaneously compensated for by *external* fluxes,
362 *e.g.*, O₂ supply, preventing a change of O₂ concentration in the system (Gnaiger 1993b).
363 Mitochondrial respiratory states monitored in closed systems satisfy the criteria of pseudo-
364 steady states for limited periods of time, when changes in the system (concentrations of O₂, fuel
365 substrates, ADP, P_i, H⁺) do not exert significant effects on metabolic fluxes (respiration,
366 phosphorylation). Such pseudo-steady states require respiratory media with sufficient buffering
367 capacity and substrates maintained at kinetically-saturating concentrations, and thus depend on
368 the kinetics of the processes under investigation.

369 **Specification of biochemical dose:** Substrates, uncouplers, inhibitors, and other
370 biochemical reagents are titrated to dissect mitochondrial function. Nominal concentrations of
371 these substances are usually reported as initial amount of substance concentration [mol·L⁻¹] in
372 the incubation medium. When aiming at the measurement of kinetically saturated processes—
373 such as OXPHOS-capacities, the concentrations for substrates can be chosen according to the
374 apparent equilibrium constant, K_m' . In the case of hyperbolic kinetics, only 80% of maximum
375 respiratory capacity is obtained at a substrate concentration of four times the K_m' , whereas
376 substrate concentrations of 5, 9, 19 and 49 times the K_m' are theoretically required for reaching
377 83%, 90%, 95% or 98% of the maximal rate (Gnaiger 2001). Other reagents are chosen to
378 inhibit or alter some processes. The amount of these chemicals in an experimental incubation
379 is selected to maximize effect, avoiding unacceptable off-target consequences that would
380 adversely affect the data being sought. Specifying the amount of substance in an incubation as
381 nominal concentration in the aqueous incubation medium can be ambiguous (Doskey *et al.*

2015), particularly for lipophilic substances (oligomycin, uncouplers, permeabilization agents) or cations (TPP⁺; fluorescent dyes such as safranin, TMRM), which accumulate in biological membranes or in the mitochondrial matrix. For example, a dose of digitonin of 8 fmol·cell⁻¹ (10 pg·cell⁻¹; 10 μg·10⁻⁶ cells) is optimal for permeabilization of endothelial cells, and the concentration in the incubation medium has to be adjusted according to the cell density applied (Doerrier *et al.* 2018).

Generally, dose/exposure can be specified per unit of biological sample, *i.e.*, (nominal moles of xenobiotic)/(number of cells) [mol·cell⁻¹] or, as appropriate, per mass of biological sample [mol·kg⁻¹]. This approach to specification of dose/exposure provides a scalable parameter that can be used to design experiments, help interpret a wide variety of experimental results, and provide absolute information that allows researchers worldwide to make the most use of published data (Doskey *et al.* 2015).

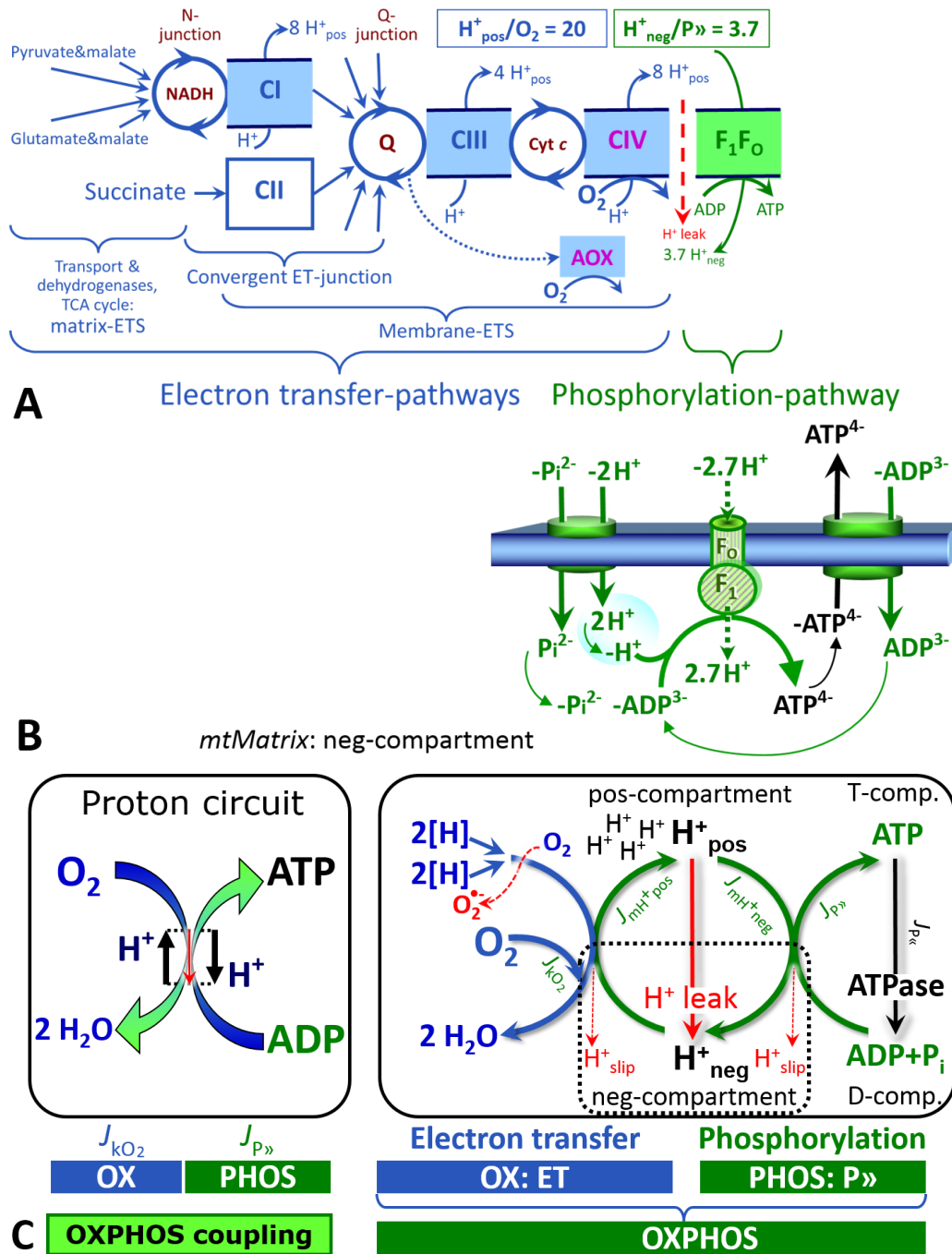
Phosphorylation, P_», and P_»/O₂ ratio: *Phosphorylation* in the context of OXPHOS is defined as phosphorylation of ADP by P_i to form ATP. On the other hand, the term phosphorylation is used generally in many contexts, *e.g.*, protein phosphorylation. This justifies consideration of a symbol more discriminating and specific than P as used in the P/O ratio (phosphate to atomic oxygen ratio), where P indicates phosphorylation of ADP to ATP or GDP to GTP. We propose the symbol P_» for the endergonic (uphill) direction of phosphorylation ADP→ATP, and likewise the symbol P_« for the corresponding exergonic (downhill) hydrolysis ATP→ADP (Fig. 2). P_» refers mainly to electrontransfer phosphorylation but may also involve substrate-level phosphorylation as part of the tricarboxylic acid (TCA) cycle (succinyl-CoA ligase; phosphoglycerate kinase) and phosphorylation of ADP catalyzed by pyruvate kinase, and of GDP phosphorylated by phosphoenolpyruvate carboxykinase. Transphosphorylation is performed by adenylate kinase, creatine kinase, hexokinase and nucleoside diphosphate kinase. In isolated mammalian mitochondria, ATP production catalyzed by adenylate kinase (2 ADP ↔ ATP + AMP) proceeds without fuel substrates in the presence of ADP (Komlódi and Tretter 2017). Kinase cycles are involved in intracellular energy transfer and signal transduction for regulation of energy flux.

The P_»/O₂ ratio (P_»/4 e⁻) is two times the ‘P/O’ ratio (P_»/2 e⁻) of classical bioenergetics. P_»/O₂ is a generalized symbol, not specific for determination of P_i consumption (P_i/O₂ flux ratio), ADP depletion (ADP/O₂ flux ratio), or ATP production (ATP/O₂ flux ratio). The mechanistic P_»/O₂ ratio or P_»/O₂ stoichiometry is calculated from the proton-to-O₂ and proton-to-phosphorylation coupling stoichiometries (Fig. 2A):

$$P_{»}/O_2 = \frac{H_{pos}^+/O_2}{H_{neg}^+/P_{»}} \quad (1)$$

The H_{pos}⁺/O₂ coupling stoichiometry (referring to the full 4 electron reduction of O₂) depends on the ET-pathway control state which defines the relative involvement of the three coupling sites (CI, CIII and CIV) in the catabolic pathway of electrons to O₂. This varies with: (1) a bypass of CI by single or multiple electron input into the Q-junction; and (2) a bypass of CIV by involvement of alternative oxidases, AOX, which are not expressed in mammalian mitochondria.

H_{pos}⁺/O₂ is 12 in the ET-pathways involving CIII and CIV as proton pumps, increasing to 20 for the NADH-pathway (Fig. 2A), but a general consensus on H_{pos}⁺/O₂ stoichiometries remains to be reached (Hinkle 2005; Wikström and Hummer 2012; Sazanov 2015). The H_{neg}⁺/P_» coupling stoichiometry (3.7; Fig. 2A) is the sum of 2.7 H_{neg}⁺ required by the F-ATPase of vertebrate and most invertebrate species (Watt *et al.* 2010) and the proton balance in the translocation of ADP, ATP and P_i (Fig. 2B). Taken together, the mechanistic P_»/O₂ ratio is calculated at 5.4 and 3.3 for NADH- and succinate-linked respiration, respectively (Eq. 1). The corresponding classical P_»/O ratios (referring to the 2 electron reduction of 0.5 O₂) are 2.7 and 1.6 (Watt *et al.* 2010), in agreement with the measured P_»/O ratio for succinate of 1.58 ± 0.02 (Gnaiger *et al.* 2000).



433
434
435
436
437
438
439
440
441
442
443
444
445

Fig. 2. Oxidative phosphorylation (OXPHOS). (A) The mitochondrial electron transfer system (ETS) is fuelled by diffusion and transport of substrates across the mtOM and mtIM and consists of the matrix-ETS and membrane-ETS. ET-pathways are coupled to the phosphorylation-pathway. ET-pathways converge at the N-junction and Q-junction. Additional arrows indicate electron entry into the Q-junction through electron transferring flavoprotein, glycerophosphate dehydrogenase, dihydro-ototate dehydrogenase, choline dehydrogenase, and sulfide-ubiquinone oxidoreductase. The dotted arrow indicates the branched pathway of oxygen consumption by alternative quinol oxidase (AOX). The H^+_{pos}/O_2 ratio is the outward proton flux from the matrix space to the positively (pos) charged compartment, divided by catabolic O_2 flux in the NADH-pathway. The H^+_{neg}/P ratio is the inward proton flux from the inter-membrane space to the negatively (neg) charged matrix space, divided by the flux of phosphorylation of ADP to ATP. These are not fixed stoichiometries due to ion leaks and proton

446 slip. (B) Phosphorylation-pathway catalyzed by the proton pump F_1F_0 -ATPase (F-ATPase,
 447 ATP synthase), adenine nucleotide translocase, and inorganic phosphate transporter. The
 448 H^+_{neg}/P_{\gg} stoichiometry is the sum of the coupling stoichiometry in the F-ATPase reaction (-2.7
 449 H^+_{pos} from the positive intermembrane space, 2.7 H^+_{neg} to the matrix, *i.e.*, the negative
 450 compartment) and the proton balance in the translocation of ADP^{2-} , ATP^{3-} and P_i^{2-} . (C) The
 451 proton circuit and coupling in OXPHOS. $2[H]$ indicates the reduced hydrogen equivalents of
 452 fuel substrates of the catabolic reaction k with oxygen. O_2 flux, J_{kO_2} , through the catabolic ET-
 453 pathway, is coupled to flux through the phosphorylation-pathway of ADP to ATP, $J_{P_{\gg}}$. The
 454 proton pumps of the ET-pathway drive proton flux into the positive (pos) compartment, J_{mH+pos} ,
 455 generating the output protonmotive force (motive, subscript m). F-ATPase is coupled to inward
 456 proton current into the negative (neg) compartment, J_{mH+neg} , to phosphorylate $ADP+P_i$ to ATP.
 457 The system defined by the boundaries (full black line) is not a black box, but is analysed as a
 458 compartmental system. The negative compartment (neg-compartment, enclosed by the dotted
 459 line) is the matrix space, separated by the mtIM from the positive compartment (pos-
 460 compartment). $ADP+P_i$ and ATP are the substrate- and product-compartments (scalar ADP and
 461 ATP compartments, D-comp. and T-comp.), respectively. At steady-state proton turnover,
 462 $J_{\infty H^+}$, and ATP turnover, $J_{\infty P}$, maintain concentrations constant, when $J_{mH+\infty} = J_{mH+pos} = J_{mH+neg}$,
 463 and $J_{P_{\infty}} = J_{P_{\gg}} = J_{P_{\ll}}$. Modified from (A) Lemieux *et al.* (2017) and (B,C) Gnaiger (2014).
 464

465 The effective P_{\gg}/O_2 flux ratio ($Y_{P_{\gg}/O_2} = J_{P_{\gg}}/J_{kO_2}$) is diminished relative to the mechanistic
 466 P_{\gg}/O_2 ratio by intrinsic and extrinsic uncoupling and dyscoupling (Fig. 3). Such generalized
 467 uncoupling is different from switching to mitochondrial pathways that involve fewer than three
 468 proton pumps ('coupling sites': Complexes CI, CIII and CIV), bypassing CI through multiple
 469 electron entries into the Q-junction, or CIII and CIV through AOX (Fig. 2). Reprogramming of
 470 mitochondrial pathways may be considered as a switch of gears (changing the stoichiometry)
 471 rather than uncoupling (loosening the stoichiometry). In addition, Y_{P_{\gg}/O_2} depends on several
 472 experimental conditions of flux control, increasing as a hyperbolic function of [ADP] to a
 473 maximum value (Gnaiger 2001).
 474

475 **Control and regulation:** The terms metabolic *control* and *regulation* are frequently used
 476 synonymously, but are distinguished in metabolic control analysis: 'We could understand the
 477 regulation as the mechanism that occurs when a system maintains some variable constant over
 478 time, in spite of fluctuations in external conditions (homeostasis of the internal state). On the
 479 other hand, metabolic control is the power to change the state of the metabolism in response to
 480 an external signal' (Fell 1997). Respiratory control may be induced by experimental control
 481 signals that *exert* an influence on: (1) ATP demand and ADP phosphorylation-rate; (2) fuel
 482 substrate composition, pathway competition; (3) available amounts of substrates and O_2 , *e.g.*,
 483 starvation and hypoxia; (4) the protonmotive force, redox states, flux-force relationships,
 484 coupling and efficiency; (5) Ca^{2+} and other ions including H^+ ; (6) inhibitors, *e.g.*, nitric oxide
 485 or intermediary metabolites such as oxaloacetate; (7) signalling pathways and regulatory
 486 proteins, *e.g.*, insulin resistance, transcription factor hypoxia inducible factor 1. *Mechanisms* of
 487 respiratory control and regulation include adjustments of: (1) enzyme activities by allosteric
 488 mechanisms and phosphorylation; (2) enzyme content, concentrations of cofactors and
 489 conserved moieties—such as adenylates, nicotinamide adenine dinucleotide [$NAD^+/NADH$],
 490 coenzyme Q, cytochrome *c*); (3) metabolic channeling by supercomplexes; and (4)
 491 mitochondrial density (enzyme concentrations and membrane area) and morphology (cristae
 492 folding, fission and fusion). Mitochondria are targeted directly by hormones, thereby affecting
 493 their energy metabolism (Lee *et al.* 2013; Gerö and Szabo 2016; Price and Dai 2016; Moreno
 494 *et al.* 2017). Evolutionary or acquired differences in the genetic and epigenetic basis of
 495 mitochondrial function (or dysfunction) between subjects and gene therapy; age; gender,
 496 biological sex, and hormone concentrations; life style including exercise and nutrition; and
 environmental issues including thermal, atmospheric, toxicological and pharmacological

497 factors, exert an influence on all control mechanisms listed above. For reviews, see Brown
498 1992; Gnaiger 1993a, 2009; 2014; Paradies *et al.* 2014; Morrow *et al.* 2017.

499 **Respiratory control and response:** Lack of control by a metabolic pathway, *e.g.*,
500 phosphorylation-pathway, means that there will be no response to a variable activating it, *e.g.*,
501 [ADP]. The reverse, however, is not true as the absence of a response to [ADP] does not exclude
502 the phosphorylation-pathway from having some degree of control. The degree of control of a
503 component of the OXPHOS-pathway on an output variable—such as O₂ flux, will in general
504 be different from the degree of control on other outputs—such as phosphorylation-flux or
505 proton leak flux. Therefore, it is necessary to be specific as to which input and output are under
506 consideration (Fell 1997).

507 **Respiratory coupling control and ET-pathway control:** Respiratory control refers to
508 the ability of mitochondria to adjust O₂ flux in response to external control signals by engaging
509 various mechanisms of control and regulation. Respiratory control is monitored in a
510 mitochondrial preparation under conditions defined as respiratory states. When
511 phosphorylation of ADP to ATP is stimulated or depressed, an increase or decrease is observed
512 in electron transfer measured as O₂ flux in respiratory coupling states of intact mitochondria
513 ('controlled states' in the classical terminology of bioenergetics). Alternatively, coupling of
514 electron transfer with phosphorylation is disengaged by uncouplers. These protonophores are
515 weak lipid-soluble acids which disrupt the barrier function of the mtIM and thus shortcircuit
516 the protonmotive system, functioning like a clutch in a mechanical system. The corresponding
517 coupling control state is characterized by a high O₂ flux without control by P» ('uncontrolled
518 state').

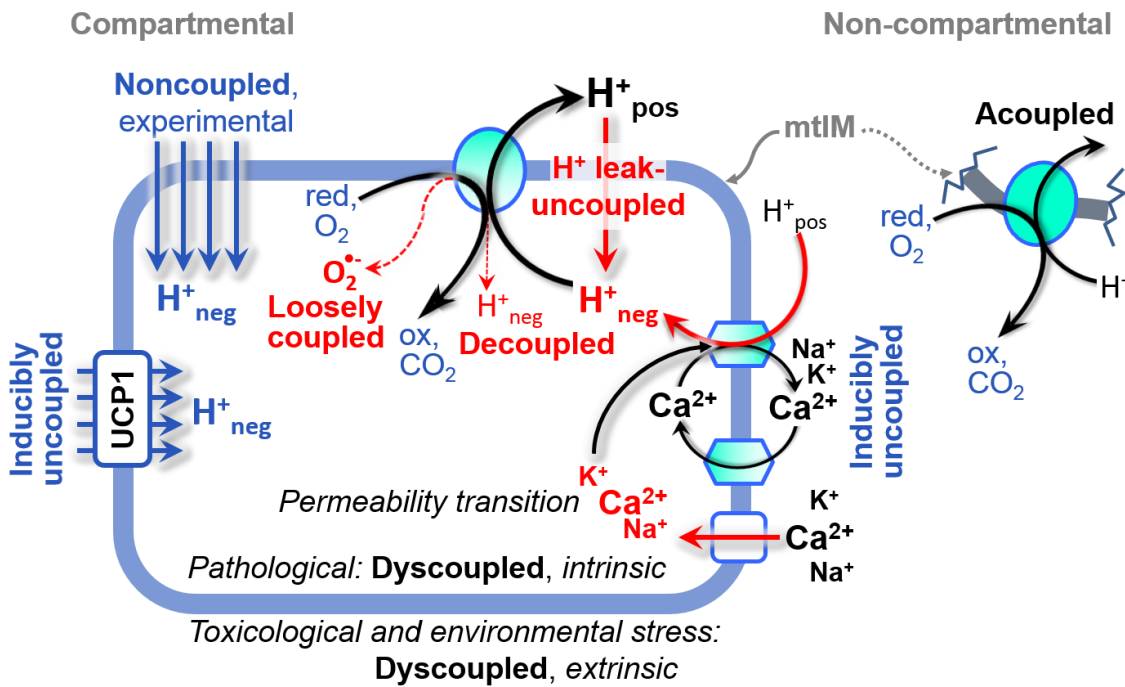
519 ET-pathway control states are obtained in mitochondrial preparations by depletion of
520 endogenous substrates and addition to the mitochondrial respiration medium of fuel substrates
521 (CHNO; 2[H] in **Fig. 2C**) and specific inhibitors, activating selected mitochondrial catabolic
522 pathways, *k* (**Fig. 2A**). Coupling control states and pathway control states are complementary,
523 since mitochondrial preparations depend on an exogenous supply of pathway-specific fuel
524 substrates and oxygen (Gnaiger 2014).

525 **Coupling:** In mitochondrial electron transfer, vectorial transmembrane proton flux is
526 coupled through the proton pumps CI, CIII and CIV to the catabolic flux of scalar reactions,
527 collectively measured as O₂ flux (**Fig. 2**). Thus mitochondria are elements of energy
528 transformation. Energy cannot be lost or produced in any internal process (First Law of
529 thermodynamics). Open and closed systems can gain or lose energy only by external fluxes—
530 by exchange with the environment. Energy is a conserved quantity. Therefore, energy can
531 neither be produced by mitochondria, nor is there any internal process without energy
532 conservation. Exergy is defined as the 'free energy' with the potential to perform work.
533 *Coupling* is the mechanistic linkage of an exergonic process (spontaneous, negative exergy
534 change) with an endergonic process (positive exergy change) in energy transformations which
535 conserve part of the exergy that would be irreversibly lost or dissipated in an uncoupled process.

536 **Uncoupling:** Uncoupling of mitochondrial respiration is a general term comprising
537 diverse mechanisms:

- 538 1. Proton leak across the mtIM from the pos- to the neg-compartment (**Fig. 2C**);
- 539 2. Cycling of other cations, strongly stimulated by permeability transition, or
540 experimentally induced by valinomycin in the presence of K⁺;
- 541 3. Proton slip in the proton pumps when protons are effectively not pumped (CI, CIII and
542 CIV) or are not driving phosphorylation (F-ATPase);
- 543 4. Loss of compartmental integrity when electron transfer is acoupled;
- 544 5. Electron leak in the loosely coupled univalent reduction of O₂ to superoxide (O₂^{-•};
545 superoxide anion radical).

546 Differences of terms—uncoupled vs. noncoupled—are easily overlooked, although they relate
547 to different meanings of uncoupling (**Fig. 3**).



548
 549 **Fig 3. Mechanisms of respiratory uncoupling.** An intact mitochondrial inner membrane,
 550 mtIM, is required for vectorial, compartmental coupling. ‘Acoupled’ respiration is the
 551 consequence of structural disruption with catalytic activity of non-compartmental
 552 mitochondrial fragments. Inducibly uncoupled (activation of UCP1) and experimentally
 553 noncoupled respiration (titration of protonophores) stimulate respiration to maximum O₂ flux.
 554 H⁺ leak-uncoupled, decoupled, and loosely coupled respiration are components of intrinsic
 555 uncoupling. Pathological dysfunction may affect all types of uncoupling, including
 556 permeability transition, causing intrinsically dyscoupled respiration. Similarly, toxicological
 557 and environmental stress factors can cause extrinsically dyscoupled respiration.

559 2.2. Coupling states and respiratory rates

560
 561 **Respiratory capacities in coupling control states:** To extend the classical nomenclature
 562 on mitochondrial coupling states (Section 2.3) by a concept-driven terminology that
 563 incorporates explicitly information on the meaning of respiratory states, the terminology must
 564 be general and not restricted to any particular experimental protocol or mitochondrial
 565 preparation (Gnaiger 2009). Concept-driven nomenclature aims at mapping the *meaning and*
 566 *concept behind* the words and acronyms onto the *forms* of words and acronyms (Miller 1991).
 567 The focus of concept-driven nomenclature is primarily the conceptual ‘why’, along with
 568 clarification of the experimental ‘how’. Respiratory capacities delineate, comparable to channel
 569 capacity in information theory (Schneider 2006), the upper bound of the rate of respiration
 570 measured in defined coupling control states and electron transfer-pathway (ET-pathway) states
 571 (**Fig. 4**).

572 To provide a diagnostic reference for respiratory capacities of core energy metabolism,
 573 the capacity of *oxidative phosphorylation*, OXPHOS, is measured at kinetically-saturating
 574 concentrations of ADP and P_i. The *oxidative ET-capacity* reveals the limitation of OXPHOS-
 575 capacity mediated by the *phosphorylation-pathway*. The ET- and phosphorylation-pathways
 576 comprise coupled segments of the OXPHOS-system. ET-capacity is measured as noncoupled
 577 respiration by application of *external uncouplers*. The contribution of *intrinsically uncoupled*
 578 O₂ consumption is studied by preventing the stimulation of phosphorylation either in the
 579 absence of ADP or by inhibition of the phosphorylation-pathway. The corresponding states are
 580 collectively classified as LEAK-states, when O₂ consumption compensates mainly for ion

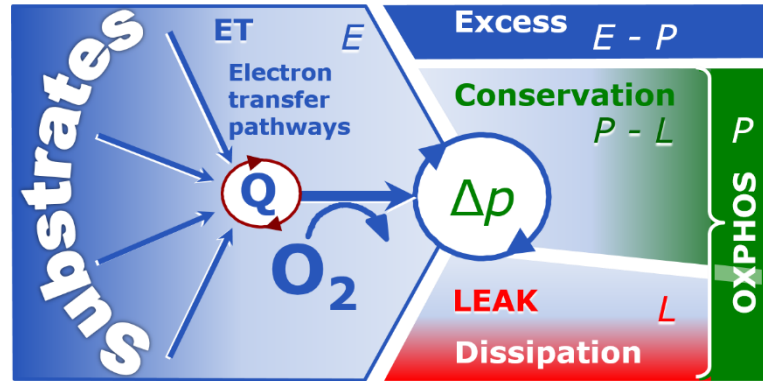
581 leaks, including the proton leak. Defined coupling states are induced by: (1) adding cation
 582 chelators such as EGTA, binding free Ca^{2+} and thus limiting cation cycling; (2) adding ADP
 583 and P_i ; (3) inhibiting the phosphorylation-pathway; and (4) uncoupler titrations, while
 584 maintaining a defined ET-pathway state with constant fuel substrates and inhibitors of specific
 585 branches of the ET-pathway (**Fig. 2A**).

586

587 **Fig. 4. Four-compartment model of oxidative phosphorylation.**

588 Respiratory states (ET, OXPHOS, LEAK; **Table 1**) and corresponding rates (E , P , L) are connected by the
 589 protonmotive force, Δp . ET-capacity, E , is partitioned into (1)
 590 dissipative LEAK-respiration, L , when the Gibbs energy change of
 591 catabolic O_2 flux is irreversibly
 592 lost, (2) net OXPHOS-capacity, $P-L$, with partial conservation of the capacity to perform work,
 593 and (3) the excess capacity, $E-P$. Modified from Gnaiger (2014).

594
 595
 596
 597
 598
 599



600

601 **Table 1. Coupling states and residual oxygen consumption in mitochondrial preparations in relation to respiration- and phosphorylation-flux, J_{O_2} and J_{P} , and protonmotive force, Δp .** Coupling states are established at kinetically-saturating concentrations of fuel substrates and O_2 .

602

603

604

State	J_{kO_2}	J_{P}	Δp	Inducing factors	Limiting factors
LEAK	L ; low, cation leak-dependent respiration	0	max.	proton leak, slip, and cation cycling	$J_{\text{P}} = 0$: (1) without ADP, L_N ; (2) max. ATP/ADP ratio, L_T ; or (3) inhibition of the phosphorylation-pathway, L_{Omy}
OXPHOS	P ; high, ADP-stimulated respiration	max.	high	kinetically-saturating [ADP] and $[\text{P}_i]$	J_{P} , by phosphorylation-pathway; or J_{kO_2} by ET-capacity
ET	E ; max., noncoupled respiration	0	low	optimal external uncoupler concentration for max. $J_{\text{O}_2, E}$	J_{kO_2} by ET-capacity
ROX	R_{ox} ; min., residual O_2 consumption	0	0	$J_{\text{O}_2, \text{Rox}}$ in non-ET-pathway oxidation reactions	full inhibition of ET-pathway; or absence of fuel substrates

605

606 The three coupling states, ET, LEAK and OXPHOS, are shown schematically with the
 607 corresponding respiratory rates, abbreviated as E , L and P , respectively (**Fig. 4**). We distinguish
 608 metabolic *pathways* from metabolic *states* and the corresponding metabolic *rates*; for example:
 609 ET-pathways (**Fig. 4**), ET-states (**Fig. 5C**), and ET-capacities, E , respectively (**Table 1**). The
 610 protonmotive force is *high* in the OXPHOS-state when it drives phosphorylation, *maximum* in
 611 the LEAK-state of coupled mitochondria, driven by LEAK-respiration at a minimum back flux

612 of cations to the matrix side, and *very low* in the ET-state when uncouplers short-circuit the
613 proton cycle (**Table 1**).

614 E may exceed or be equal to P . $E > P$ is observed in many types of mitochondria, varying
615 between species, tissues and cell types (Gnaiger 2009). $E-P$ is the excess ET-capacity pushing
616 the phosphorylation-flux (**Fig. 2B**) to the limit of its *capacity of utilizing* the protonmotive force.
617 In addition, the magnitude of $E-P$ depends on the tightness of respiratory coupling or degree of
618 uncoupling, since an increase of L causes P to increase towards the limit of E . The *excess* $E-P$
619 capacity, $E-P$, therefore, provides a sensitive diagnostic indicator of specific injuries of the
620 phosphorylation-pathway, under conditions when E remains constant but P declines relative to
621 controls (**Fig. 4**). Substrate cocktails supporting simultaneous convergent electron transfer to
622 the Q-junction for reconstitution of TCA cycle function establish pathway control states with
623 high ET-capacity, and consequently increase the sensitivity of the $E-P$ assay.

624 E cannot theoretically be lower than P . $E < P$ must be discounted as an artefact, which
625 may be caused experimentally by: (1) loss of oxidative capacity during the time course of the
626 respirometric assay, since E is measured subsequently to P ; (2) using insufficient uncoupler
627 concentrations; (3) using high uncoupler concentrations which inhibit ET (Gnaiger 2008); (4)
628 high oligomycin concentrations applied for measurement of L before titrations of uncoupler,
629 when oligomycin exerts an inhibitory effect on E . On the other hand, the excess ET-capacity is
630 overestimated if non-saturating [ADP] or [P_i] are used. See State 3 in the next section.

631 The net OXPHOS-capacity is calculated by subtracting L from P (**Fig. 4**). Then the net
632 $P \gg O_2$ equals $P \gg (P-L)$, wherein the dissipative LEAK component in the OXPHOS-state
633 be overestimated. This can be avoided by measuring LEAK-respiration in a state when the
634 protonmotive force is adjusted to its slightly lower value in the OXPHOS-state—by titration of
635 an ET inhibitor (Divakaruni and Brand 2011). Any turnover-dependent components of proton
636 leak and slip, however, are underestimated under these conditions (Garlid *et al.* 1993). In
637 general, it is inappropriate to use the term *ATP production* or *ATP turnover* for the difference
638 of O₂ flux measured in states P and L . The difference $P-L$ is the upper limit of the part of
639 OXPHOS-capacity that is freely available for ATP production (corrected for LEAK-
640 respiration) and is fully coupled to phosphorylation with a maximum mechanistic stoichiometry
641 (**Fig. 4**).

642
643 **LEAK-state (Fig. 5A):** The LEAK-state is defined as a state of mitochondrial respiration
644 when O₂ flux mainly compensates for ion leaks in the absence of ATP synthesis, at kinetically-
645 saturating concentrations of O₂ and respiratory fuel substrates. LEAK-respiration is measured
646 to obtain an estimate of *intrinsic uncoupling* without addition of an experimental uncoupler: (1)
647 in the absence of adenylates; (2) after depletion of ADP at a maximum ATP/ADP ratio; or (3)
648 after inhibition of the phosphorylation-pathway by inhibitors of F-ATPase—such as
649 oligomycin, or of adenine nucleotide translocase—such as carboxyatractyloside. Adjustment
650 of the nominal concentration of these inhibitors to the density of biological sample applied can
651 minimize or avoid inhibitory side-effects exerted on ET-capacity or even some dyscoupling.

652 **Proton leak and uncoupled respiration:** Proton leak is a leak current of protons. The
653 intrinsic proton leak is the *uncoupled* process in which protons diffuse across the mtIM in the
654 dissipative direction of the downhill protonmotive force without coupling to phosphorylation
655 (**Fig. 5A**). The proton leak flux depends non-linearly on the protonmotive force (Garlid *et al.*
656 1989; Divakaruni and Brand 2011), it is a property of the mtIM and may be enhanced due to
657 possible contaminations by free fatty acids. Inducible uncoupling mediated by uncoupling
658 protein 1 (UCP1) is physiologically controlled, *e.g.*, in brown adipose tissue. UCP1 is a member
659 of the mitochondrial carrier family which is involved in the translocation of protons across the
660 mtIM (Klingenberg 2017). Consequently, the short-circuit diminishes the protonmotive force
661 and stimulates electron transfer to O₂ and heat dissipation without phosphorylation of ADP.
662

663 **Cation cycling:** There can
 664 be other cation contributors to
 665 leak current including calcium
 666 and probably magnesium.
 667 Calcium current is balanced by
 668 mitochondrial $\text{Na}^+/\text{Ca}^{2+}$
 669 exchange, which is balanced by
 670 Na^+/H^+ or K^+/H^+ exchanges. This
 671 is another effective uncoupling
 672 mechanism different from proton
 673 leak (**Table 2**).

674 **Proton slip and**
 675 **decoupled respiration:** Proton
 676 slip is the *decoupled* process in
 677 which protons are only partially
 678 translocated by a proton pump of
 679 the ET-pathways and slip back to
 680 the original compartment. The
 681 proton leak is the dominant
 682 contributor to the overall leak
 683 current in mammalian
 684 mitochondria incubated under
 685 physiological conditions at 37
 686 °C, whereas proton slip is
 687 increased at lower experimental
 688 temperature (Canton *et al.* 1995).
 689 Proton slip can also happen in
 690 association with the F-ATPase, in
 691 which the proton slips downhill
 692 across the pump to the matrix
 693 without contributing to ATP
 694 synthesis. In each case, proton
 695 slip is a property of the proton
 696 pump and increases with the
 697 pump turnover rate.

698 **Electron leak and loosely**
 699 **coupled respiration:**
 700 Superoxide production by the
 701 ETS leads to a bypass of proton
 702 pumps and correspondingly
 703 lower $\text{P}_{\gg}/\text{O}_2$ ratio. This depends
 704 on the actual site of electron leak
 705 and the scavenging of hydrogen peroxide by cytochrome *c*, whereby electrons may re-enter the
 706 ETS with proton translocation by CIV.

707 **Loss of compartmental integrity and acoupled respiration:** Electron transfer and
 708 catabolic O_2 flux proceed without compartmental proton translocation in disrupted
 709 mitochondrial fragments. Such fragments form during mitochondrial isolation, and may not
 710 fully fuse to re-establish structurally intact mitochondria. Loss of mtIM integrity, therefore, is
 711 the cause of acoupled respiration, which is a nonvectorial dissipative process without control
 712 by the protonmotive force.

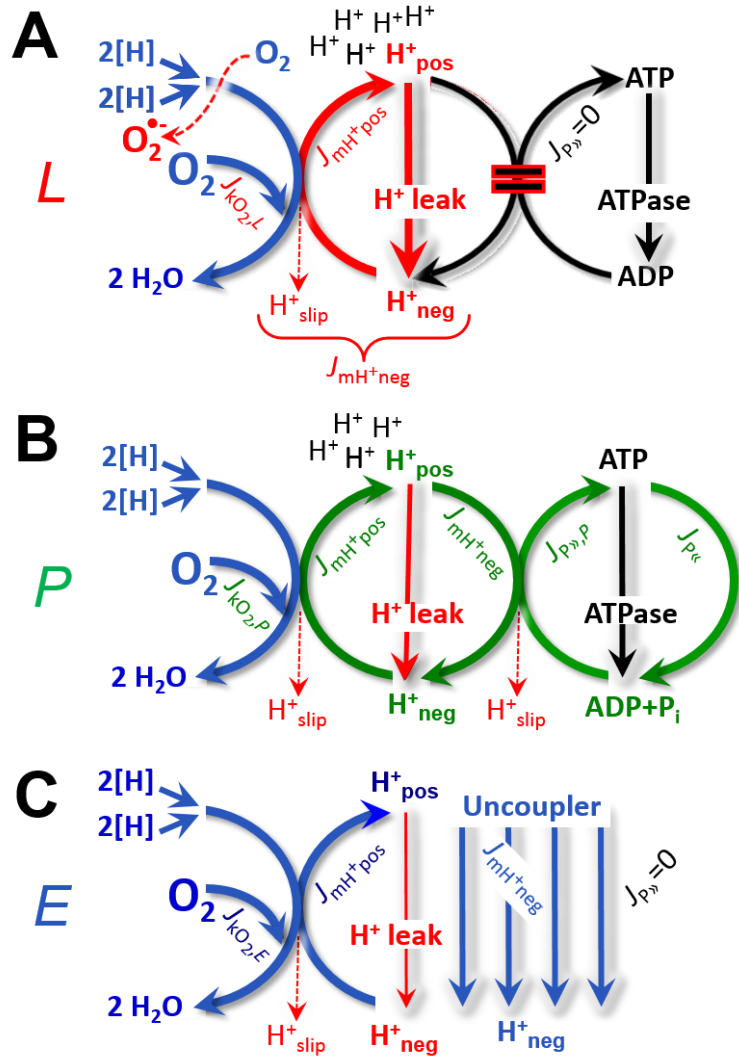


Fig. 5. Respiratory coupling states. A: LEAK-state and rate, L: Phosphorylation is arrested, $J_{\text{P}_{\gg}} = 0$, and catabolic O_2 flux, $J_{\text{KO}_2, \text{L}}$, is controlled mainly by the proton leak, $J_{\text{mH}^+ \text{neg}, \text{L}}$, at maximum protonmotive force (**Fig. 3**). **B: OXPHOS-state and rate, P:** Phosphorylation, $J_{\text{P}_{\gg}}$, is stimulated by kinetically-saturating [ADP] and $[\text{P}_i]$, and is supported by a high protonmotive force. O_2 flux, $J_{\text{KO}_2, \text{P}}$, is well-coupled at a $\text{P}_{\gg}/\text{O}_2$ ratio of $J_{\text{P}_{\gg}, \text{P}}/J_{\text{O}_2, \text{P}}$. **C: ET-state and rate, E:** Noncoupled respiration, $J_{\text{KO}_2, \text{E}}$, is maximum at optimum exogenous uncoupler concentration and phosphorylation is zero, $J_{\text{P}_{\gg}} = 0$. See also **Fig. 2**.

713 **Dyscoupled respiration:** Mitochondrial injuries may lead to *dyscoupling* as a
 714 pathological or toxicological cause of *uncoupled* respiration. Dyscoupling may involve any
 715 type of uncoupling mechanism, *e.g.*, opening the permeability transition pore. Dyscoupled
 716 respiration is distinguished from the experimentally induced *noncoupled* respiration in the ET-
 717 state (**Table 2**).

718
 719

Table 2. Terms on respiratory coupling and uncoupling.

Term	$J_{\text{K}\text{O}_2}$	$P \gg O_2$	Note	
acoupled		0	electron transfer in mitochondrial fragments without vectorial proton translocation (Fig. 3)	
intrinsic, no protonophore added	uncoupled	L	0	non-phosphorylating LEAK-respiration (Fig. 5A)
	proton leak-uncoupled		0	component of L , H^+ diffusion across the mtIM (Fig. 3)
	decoupled		0	component of L , proton slip (Fig. 3)
	loosely coupled		0	component of L , lower coupling due to superoxide formation and bypass of proton pumps (Fig. 3)
	dyscoupled		0	pathologically, toxicologically, environmentally increased uncoupling, mitochondrial dysfunction
	inducibly uncoupled		0	by UCP1 or cation (<i>e.g.</i> , Ca^{2+}) cycling (Fig. 3)
noncoupled	E	0	non-phosphorylating respiration stimulated to maximum flux at optimum exogenous uncoupler concentration (Fig. 5C)	
well-coupled	P	high	phosphorylating respiration with an intrinsic LEAK component (Fig. 5B)	
fully coupled	$P - L$	max.	OXPPOS-capacity corrected for LEAK-respiration (Fig. 4)	

720

721 **OXPPOS-state (Fig. 5B):** The OXPPOS-state is defined as the respiratory state with
 722 kinetically-saturating concentrations of O_2 , respiratory and phosphorylation substrates, and
 723 absence of exogenous uncoupler, which provides an estimate of the maximal respiratory
 724 capacity in the OXPPOS-state for any given ET-pathway state. Respiratory capacities at
 725 kinetically-saturating substrate concentrations provide reference values or upper limits of
 726 performance, aiming at the generation of data sets for comparative purposes. Physiological
 727 activities and effects of substrate kinetics can be evaluated relative to the OXPPOS-capacity.

728 As discussed previously, 0.2 mM ADP does not fully saturate flux in isolated
 729 mitochondria (Gnaiger 2001; Puchowicz *et al.* 2004); greater ADP concentration is required,
 730 particularly in permeabilized muscle fibres and cardiomyocytes, to overcome limitations by
 731 intracellular diffusion and by the reduced conductance of the mtOM (Jepihhina *et al.* 2011,
 732 Illaste *et al.* 2012, Simson *et al.* 2016), either through interaction with tubulin (Rostovtseva *et al.* 2008) or other intracellular structures (Birkedal *et al.* 2014). In permeabilized muscle fibre
 733 bundles of high respiratory capacity, the apparent K_m for ADP increases up to 0.5 mM (Saks *et al.* 1998), consistent with experimental evidence that >90% saturation is reached only at >5
 734 mM ADP (Pesta and Gnaiger 2012). Similar ADP concentrations are also required for accurate
 735 determination of OXPPOS-capacity in human clinical cancer samples and permeabilized cells
 736 (Klepinin *et al.* 2016; Koit *et al.* 2017). Whereas 2.5 to 5 mM ADP is sufficient to obtain the
 737
 738

739 actual OXPHOS-capacity in many types of permeabilized tissue and cell preparations,
740 experimental validation is required in each specific case.

741

742 **Electron transfer-state (Fig. 5C):** The ET-state is defined as the *noncoupled* state with
743 kinetically-saturating concentrations of O₂, respiratory substrate and optimum *exogenous*
744 uncoupler concentration for maximum O₂ flux. O₂ flux determined in the ET-state yields an
745 estimate of ET-capacity. Inhibition of respiration is observed above optimum uncoupler
746 concentrations. As a consequence of the nearly collapsed protonmotive force, the driving force
747 is insufficient for phosphorylation, and $J_{P_{\gg}} = 0$.

748

749 **ROX state and *Rox*:** Besides the three fundamental coupling states of mitochondrial
750 preparations, the state of residual O₂ consumption, ROX, is relevant to assess respiratory
751 function. ROX is not a coupling state. The rate of residual oxygen consumption, *Rox*, is defined
752 as O₂ consumption due to oxidative reactions measured after inhibition of ET— with rotenone,
753 malonic acid and antimycin A. Cyanide and azide inhibit CIV and several peroxidases involved
754 in *Rox*. High concentrations of antimycin A also inhibit peroxisomal acyl-CoA oxidase and D-
755 amino acid oxidase (Vamecq *et al.* 1987). ROX represents a baseline that is used to correct
756 respiration in defined coupling states. *Rox* is not necessarily equivalent to non-mitochondrial
757 reduction of O₂, considering O₂-consuming reactions in mitochondria that are not related to
758 ET— such as O₂ consumption in reactions catalyzed by monoamine oxidases (type A and B),
759 monooxygenases (cytochrome P450 monooxygenases), dioxygenase (sulfur dioxygenase and
760 trimethyllysine dioxygenase), and several hydroxylases. Mitochondrial preparations, especially
761 those obtained from liver, may be contaminated by peroxisomes. This fact makes the exact
762 determination of mitochondrial O₂ consumption and mitochondria-associated generation of
763 reactive oxygen species complicated (Schönfeld *et al.* 2009; Speijer 2016; Fig. 1). The
764 dependence of ROX-linked O₂ consumption needs to be studied in detail together with non-ET
765 enzyme activities, availability of specific substrates, O₂ concentration, and electron leakage
766 leading to the formation of reactive oxygen species.

767

768 2.3. Classical terminology for isolated mitochondria

769 ‘When a code is familiar enough, it ceases appearing like a code; one forgets that there
770 is a decoding mechanism. The message is identical with its meaning’ (Hofstadter 1979).

771

772 Chance and Williams (1955; 1956) introduced five classical states of mitochondrial
773 respiration and cytochrome redox states. Table 3 shows a protocol with isolated mitochondria
774 in a closed respirometric chamber, defining a sequence of respiratory states. States and rates
775 are not specifically distinguished in this nomenclature.

776 **State 1** is obtained after addition of isolated mitochondria to air-saturated
777 isoosmotic/isotonic respiration medium containing P_i, but no fuel substrates and no adenylates,
778 *i.e.*, AMP, ADP, ATP.

779 **State 2** is induced by addition of a ‘high’ concentration of ADP (typically 100 to 300
780 μM), which stimulates respiration transiently on the basis of endogenous fuel substrates and
781 phosphorylates only a small portion of the added ADP. State 2 is then obtained at a low
782 respiratory activity limited by exhausted endogenous fuel substrate availability (Table 3). If
783 addition of specific inhibitors of respiratory complexes— such as rotenone— does not cause a
784 further decline of O₂ flux, State 2 is equivalent to the ROX state (See below.). If inhibition is
785 observed, undefined endogenous fuel substrates are a confounding factor of pathway control,
786 contributing to the effect of subsequently externally added substrates and inhibitors. In contrast
787 to the original protocol, an alternative sequence of titration steps is frequently applied, in which
788 the alternative ‘State 2’ has an entirely different meaning, when this second state is induced by

789 addition of fuel substrate without ADP (LEAK-state; in contrast to State 2 defined in **Table 1**
790 as a ROX state), followed by addition of ADP.

791
792
793
794

Table 3. Metabolic states of mitochondria (Chance and Williams, 1956; Table V).

State	[O ₂]	ADP level	Substrate level	Respiration rate	Rate-limiting substance
1	>0	Low	low	slow	ADP
2	>0	high	~0	slow	substrate
3	>0	high	high	fast	respiratory chain
4	>0	Low	high	slow	ADP
5	0	high	high	0	oxygen

795

796 **State 3** is the state stimulated by addition of fuel substrates while the ADP concentration
797 is still high (**Table 3**) and supports coupled energy transformation through oxidative
798 phosphorylation. 'High ADP' is a concentration of ADP specifically selected to allow the
799 measurement of State 3 to State 4 transitions of isolated mitochondria in a closed respirometric
800 chamber. Repeated ADP titration re-establishes State 3 at 'high ADP'. Starting at O₂
801 concentrations near air-saturation (ca. 200 μM O₂ at sea level and 37 °C), the total ADP
802 concentration added must be low enough (typically 100 to 300 μM) to allow phosphorylation
803 to ATP at a coupled O₂ flux that does not lead to O₂ depletion during the transition to State 4.
804 In contrast, kinetically-saturating ADP concentrations usually are 10-fold higher than 'high
805 ADP', e.g., 2.5 mM in isolated mitochondria. The abbreviation State 3u is occasionally used in
806 bioenergetics, to indicate the state of respiration after titration of an uncoupler, without
807 sufficient emphasis on the fundamental difference between OXPHOS-capacity (*well-coupled*
808 with an *endogenous* uncoupled component) and ET-capacity (*noncoupled*).

809 **State 4** is a LEAK-state that is obtained only if the mitochondrial preparation is intact
810 and well-coupled. Depletion of ADP by phosphorylation to ATP causes a decline of O₂ flux in
811 the transition from State 3 to State 4. Under the conditions of State 4, a maximum protonmotive
812 force and high ATP/ADP ratio are maintained. The gradual decline of Y_{P_{\gg}/O_2} towards
813 diminishing [ADP] at State 4 must be taken into account for calculation of P_{\gg}/O_2 ratios (Gnaiger
814 2001). State 4 respiration, L_T (**Table 1**), reflects intrinsic proton leak and ATP hydrolysis
815 activity. O₂ flux in State 4 is an overestimation of LEAK-respiration if the contaminating ATP
816 hydrolysis activity recycles some ATP to ADP, $J_{P_{\ll}}$, which stimulates respiration coupled to
817 phosphorylation, $J_{P_{\gg}} > 0$. This can be tested by inhibition of the phosphorylation-pathway using
818 oligomycin, ensuring that $J_{P_{\gg}} = 0$ (State 4o). Alternatively, sequential ADP titrations re-
819 establish State 3, followed by State 3 to State 4 transitions while sufficient O₂ is available.
820 Anoxia may be reached, however, before exhaustion of ADP (State 5).

821 **State 5** is the state after exhaustion of O₂ in a closed respirometric chamber. Diffusion of
822 O₂ from the surroundings into the aqueous solution may be a confounding factor preventing
823 complete anoxia (Gnaiger 2001). Chance and Williams (1955) provide an alternative definition
824 of State 5, which gives it the different meaning of ROX versus anoxia: 'State 5 may be obtained
825 by antimycin A treatment or by anaerobiosis'.

826 In **Table 3**, only States 3 and 4 (and 'State 2' in the alternative protocol: addition of fuel
827 substrates without ADP; not included in the table) are coupling control states, with the
828 restriction that O₂ flux in State 3 may be limited kinetically by non-saturating ADP
829 concentrations (**Table 1**).

830

831

832

833 3. Normalization: fluxes and flows

834

835 3.1. Normalization: system or sample

836

837

838

839

840

The term *rate* is not sufficiently defined to be useful for reporting data (**Fig. 6**). The inconsistency of the meanings of rate becomes fully apparent when considering Galileo Galilei's famous principle, that 'bodies of different weight all fall at the same rate (have a constant acceleration)' (Coopersmith 2010).

841

842

843

844

845

Flow per system, I : In a generalization of electrical terms, flow as an extensive quantity (I ; per system) is distinguished from flux as a size-specific quantity (J ; per system size) (**Fig. 6**). Electric current is flow, I_{el} [$A \equiv C \cdot s^{-1}$] per system (extensive quantity). When dividing this extensive quantity by system size (cross-sectional area of a 'wire'), a size-specific quantity is obtained, which is flux (current density), J_{el} [$A \cdot m^{-2} = C \cdot s^{-1} \cdot m^{-2}$].

846

847

848

849

Extensive quantities: An extensive quantity increases proportionally with system size. The magnitude of an extensive quantity is completely additive for non-interacting subsystems—such as mass or flow expressed per defined system. The magnitude of these quantities depends on the extent or size of the system (Cohen *et al.* 2008).

850

851

852

853

854

855

856

857

858

Size-specific quantities: 'The adjective *specific* before the name of an extensive quantity is often used to mean *divided by mass*' (Cohen *et al.* 2008). In this system-paradigm, mass-specific flux is flow divided by mass of the *system* (the total mass of everything within the measuring chamber or reactor). A mass-specific quantity is independent of the extent of non-interacting homogenous subsystems. Tissue-specific quantities (related to the *sample* in contrast to the *system*) are of fundamental interest in the field of comparative mitochondrial physiology, where *specific* refers to the *type of the sample* rather than *mass of the system*. The term *specific*, therefore, must be clarified; *sample-specific*, *e.g.*, muscle mass-specific normalization, is distinguished from *system-specific* quantities (mass or volume; **Fig. 6**).

859

860 **Fig. 6. Different meanings of rate may lead to confusion, if the normalization is not sufficiently specified.**

861

862

863

864

865

866

867

868

869

870

871

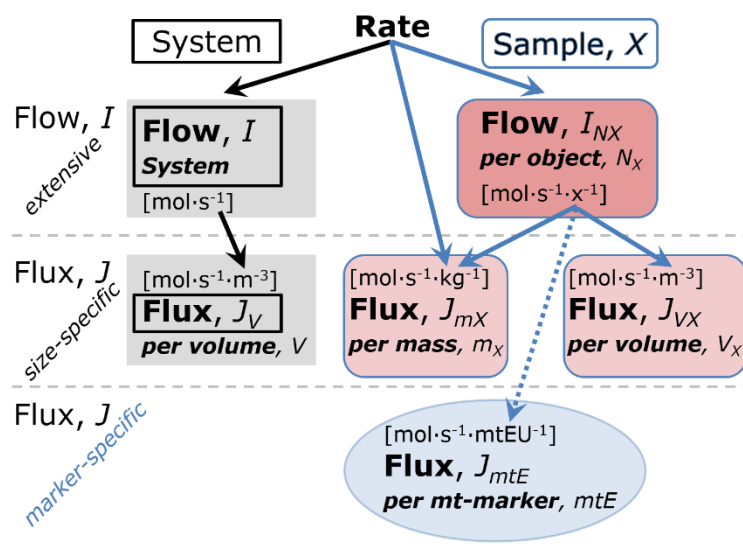
872

873

874

875

876



875

876

877 **Box 2: Metabolic fluxes and flows: vectorial and scalar**

878

879

880

881

882

883

Fluxes are *vectors*, if they have *spatial* geometric direction in addition to magnitude. Electric charge per unit time is electric flow or current, $I_{el} = dQ_{el} \cdot dt^{-1}$ [A]. When expressed per unit cross-sectional area, A [m^2], a vector flux is obtained, which is current density or surface-density of flow) perpendicular to the direction of flux, $J_{el} = I_{el} \cdot A^{-1}$ [$A \cdot m^{-2}$] (Cohen *et al.* 2008). For all transformations *flows*, I_{tr} , are defined as extensive quantities. Vector and scalar *fluxes*

884 are obtained as $J_{tr} = I_{tr} \cdot A^{-1}$ [$\text{mol} \cdot \text{s}^{-1} \cdot \text{m}^{-2}$] and $J_{tr} = I_{tr} \cdot V^{-1}$ [$\text{mol} \cdot \text{s}^{-1} \cdot \text{m}^{-3}$], expressing flux as an area-
 885 specific vector or volume-specific vectorial or scalar quantity, respectively (Gnaiger 1993b).

886 We suggest to define: (1) *vectorial* fluxes, which are translocations as functions of
 887 *gradients* with direction in geometric space in continuous systems; (2) *vectorial* fluxes, which
 888 describe translocations in discontinuous systems and are restricted to information on
 889 *compartmental differences* (**Fig. 2C**, transmembrane proton flux); and (3) *scalar* fluxes, which
 890 are transformations in a *homogenous* system (**Fig. 2C**, catabolic O₂ flux, J_{kO_2}).

891 Vectorial transmembrane proton fluxes, $J_{\text{mH}^+\text{pos}}$ and $J_{\text{mH}^+\text{neg}}$, are analyzed in a
 892 heterogenous compartmental system as a quantity with *directional* but not *spatial* information.
 893 Translocation of protons across the mtIM has a defined direction, either from the negative
 894 compartment (matrix space; negative, neg–compartment) to the positive compartment (inter-
 895 membrane space; positive, pos–compartment) or *vice versa* (**Fig. 2C**). The arrows defining the
 896 direction of the translocation between the two compartments may point upwards or downwards,
 897 right or left, without any implication that these are actual directions in space. The pos–
 898 compartment is neither above nor below the neg–compartment in a spatial sense, but can be
 899 visualized arbitrarily in a figure in the upper position (**Fig. 2C**). In general, the *compartmental*
 900 *direction* of vectorial translocation from the neg–compartment to the pos–compartment is
 901 defined by assigning the initial and final state as *ergodynamic compartments*, $\text{H}^+_{\text{neg}} \rightarrow \text{H}^+_{\text{pos}}$ or
 902 $0 = -1 \text{H}^+_{\text{neg}} + 1 \text{H}^+_{\text{pos}}$, related to work (erg = work) that must be performed to lift the proton from
 903 a lower to a higher electrochemical potential or from the lower to the higher ergodynamic
 904 compartment (Gnaiger 1993b).

905 In analogy to *vectorial* translocation, the direction of a *scalar* chemical reaction, $\text{A} \rightarrow \text{B}$
 906 or $0 = -1 \text{A} + 1 \text{B}$, is defined by assigning substrates and products, A and B, as ergodynamic
 907 compartments. O₂ is defined as a substrate in respiratory O₂ consumption, which together with
 908 the fuel substrates comprises the substrate compartment of the catabolic reaction. Volume-
 909 specific scalar O₂ flux is coupled to vectorial translocation, yielding the $\text{H}^+_{\text{pos}}/\text{O}_2$ ratio (**Fig. 2**).
 910

911

912 3.2. Normalization for system-size: flux per chamber volume

913

914 **System-specific flux, J_{V,O_2} :** The experimental system (experimental chamber) is part of
 915 the measurement apparatus, separated from the environment as an isolated, closed, open,
 916 isothermal or non-isothermal system (**Table 4**). On another level, we distinguish between (1)
 917 the *system* with volume V and mass m defined by the system boundaries, and (2) the *sample* or
 918 *objects* with volume V_X and mass m_X which are enclosed in the experimental chamber (**Fig. 6**).
 919 Metabolic O₂ flow per object, $I_{\text{O}_2/X}$, increases as the mass of the object is increased. Sample
 920 mass-specific O₂ flux, $J_{\text{O}_2/mX}$ should be independent of the mass of the sample studied in the
 921 instrument chamber, but system volume-specific O₂ flux, J_{V,O_2} (per volume of the instrument
 922 chamber), should increase in direct proportion to the mass of the sample in the chamber.
 923 Whereas J_{V,O_2} depends on mass-concentration of the sample in the chamber, it should be
 924 independent of the chamber (system) volume at constant sample mass. There are practical
 925 limitations to increase the mass-concentration of the sample in the chamber, when one is
 926 concerned about crowding effects and instrumental time resolution.

927 When the reactor volume does not change during the reaction, which is typical for liquid
 928 phase reactions, the volume-specific *flux of a chemical reaction* r is the time derivative of the
 929 advancement of the reaction per unit volume, $J_{V,rB} = d_r \zeta_B / dt \cdot V^{-1}$ [$(\text{mol} \cdot \text{s}^{-1}) \cdot \text{L}^{-1}$]. The *rate of*
 930 *concentration change* is dc_B / dt [$(\text{mol} \cdot \text{L}^{-1}) \cdot \text{s}^{-1}$], where concentration is $c_B = n_B / V$. There is a
 931 difference between (1) $J_{V,r\text{O}_2}$ [$\text{mol} \cdot \text{s}^{-1} \cdot \text{L}^{-1}$] and (2) rate of concentration change [$\text{mol} \cdot \text{L}^{-1} \cdot \text{s}^{-1}$].
 932 These merge to a single expression only in closed systems. In open systems, external fluxes
 933 (such as O₂ supply) are distinguished from internal transformations (catabolic flux, O₂
 934 consumption). In a closed system, external flows of all substances are zero and O₂ consumption

935 (internal flow of catabolic reactions k), I_{kO_2} [$\text{pmol}\cdot\text{s}^{-1}$], causes a decline of the amount of O_2 in
 936 the system, n_{O_2} [nmol]. Normalization of these quantities for the volume of the system, V [$\text{L} \equiv$
 937 dm^3], yields volume-specific O_2 flux, $J_{V,kO_2} = I_{kO_2}/V$ [$\text{nmol}\cdot\text{s}^{-1}\cdot\text{L}^{-1}$], and O_2 concentration, $[O_2]$
 938 or $c_{O_2} = n_{O_2}/V$ [$\mu\text{mol}\cdot\text{L}^{-1} = \mu\text{M} = \text{nmol}\cdot\text{mL}^{-1}$]. Instrumental background O_2 flux is due to external
 939 flux into a non-ideal closed respirometer; then total volume-specific flux has to be corrected for
 940 instrumental background O_2 flux— O_2 diffusion into or out of the instrumental chamber. J_{V,kO_2}
 941 is relevant mainly for methodological reasons and should be compared with the accuracy of
 942 instrumental resolution of background-corrected flux, *e.g.*, $\pm 1 \text{ nmol}\cdot\text{s}^{-1}\cdot\text{L}^{-1}$ (Gnaiger 2001).
 943 ‘Metabolic’ or catabolic indicates O_2 flux, J_{kO_2} , corrected for: (1) instrumental background O_2
 944 flux; (2) chemical background O_2 flux due to autoxidation of chemical components added to
 945 the incubation medium; and (3) R_{ox} for O_2 -consuming side reactions unrelated to the catabolic
 946 pathway k .

947

948 3.3. Normalization: per sample

949

950 The challenges of measuring mitochondrial respiratory flux are matched by those of
 951 normalization. Application of common and defined units is required for direct transfer of
 952 reported results into a database. The second [s] is the *SI* unit for the base quantity *time*. It is also
 953 the standard time-unit used in solution chemical kinetics. A rate may be considered as the
 954 numerator and normalization as the complementary denominator, which are tightly linked in
 955 reporting the measurements in a format commensurate with the requirements of a database.
 956 Normalization (**Table 4**) is guided by physicochemical principles, methodological
 957 considerations, and conceptual strategies (**Fig. 7**).

958 **Sample concentration, C_{mX} :** Normalization for sample concentration is required to
 959 report respiratory data. Considering a tissue or cells as the sample, X , the sample mass is m_X
 960 [mg], which is frequently measured as wet or dry weight, W_w or W_d [mg], respectively, or as
 961 amount of tissue or cell protein, m_{Protein} . In the case of permeabilized tissues, cells, and
 962 homogenates, the sample concentration, $C_{mX} = m_X/V$ [$\text{g}\cdot\text{L}^{-1} = \text{mg}\cdot\text{mL}^{-1}$], is the mass of the
 963 subsample of tissue that is transferred into the instrument chamber.

964 **Mass-specific flux, $J_{O_2/mX}$:** Mass-specific flux is obtained by expressing respiration per
 965 mass of sample, m_X [mg]. X is the type of sample—isolated mitochondria, tissue homogenate,
 966 permeabilized fibres or cells. Volume-specific flux is divided by mass concentration of X , $J_{O_2/mX}$
 967 $= J_{V,O_2}/C_{mX}$; or flow per cell is divided by mass per cell, $J_{O_2/m\text{cell}} = I_{O_2/\text{cell}}/M_{\text{cell}}$. If mass-specific
 968 O_2 flux is constant and independent of sample size (expressed as mass), then there is no
 969 interaction between the subsystems. A 1.5 mg and a 3.0 mg muscle sample respire at identical
 970 mass-specific flux. Mass-specific O_2 flux, however, may change with the mass of a tissue
 971 sample, cells or isolated mitochondria in the measuring chamber, in which the nature of the
 972 interaction becomes an issue. Therefore, cell density must be optimized, particularly in
 973 experiments carried out in wells, considering the confluency of the cell monolayer or clumps
 974 of cells (Salabei *et al.* 2014).

975 **Number concentration, C_{NX} :** C_{NX} is the experimental *number concentration* of sample
 976 X . In the case of cells or animals, *e.g.*, nematodes, $C_{NX} = N_X/V$ [$\text{x}\cdot\text{L}^{-1}$], where N_X is the number
 977 of cells or organisms in the chamber (**Table 4**).

978 **Flow per object, $I_{O_2/X}$:** A special case of normalization is encountered in respiratory
 979 studies with permeabilized (or intact) cells. If respiration is expressed per cell, the O_2 flow per
 980 measurement system is replaced by the O_2 flow per cell, $I_{O_2/\text{cell}}$ (**Table 4**). O_2 flow can be
 981 calculated from volume-specific O_2 flux, J_{V,O_2} [$\text{nmol}\cdot\text{s}^{-1}\cdot\text{L}^{-1}$] (per V of the measurement chamber
 982 [L]), divided by the number concentration of cells, $C_{N\text{cell}} = N_{\text{cell}}/V$ [$\text{cell}\cdot\text{L}^{-1}$], where N_{cell} is the
 983 number of cells in the chamber. The total cell count is the sum of viable and dead cells, $N_{\text{cell}} =$
 984 $N_{\text{vce}} + N_{\text{dce}}$ (**Table 5**). The cell viability index, $\text{CVI} = N_{\text{vce}}/N_{\text{cell}}$, is the ratio of viable cells (N_{vce} ;
 985 before experimental permeabilization) per total cell count. After experimental permeabilization,

986 all cells are permeabilized, $N_{pce} = N_{cell}$. The cell viability index can be used to normalize
 987 respiration for the number of cells that have been viable before experimental permeabilization,
 988 $I_{O_2/vce} = I_{O_2/cell}/CVI$, considering that mitochondrial respiratory dysfunction in dead cells should
 989 be eliminated as a confounding factor.

990
 991
 992

Table 4. Sample concentrations and normalization flux.

Expression	Symbol	Definition	Unit	Notes
Sample				
identity of sample	X	object: cell, tissue, animal, patient		
number of sample entities X	N_X	number of objects	x	
mass of sample X	m_X		kg	1
mass of object X	M_X	$M_X = m_X \cdot N_X^{-1}$	$kg \cdot x^{-1}$	1
Mitochondria				
mitochondria	mt	$X = mt$		
amount of mt-elements	mtE	quantity of mt-marker	mtEU	
Concentrations				
object number concentration	C_{NX}	$C_{NX} = N_X \cdot V^{-1}$	$x \cdot m^{-3}$	2
sample mass concentration	C_{mX}	$C_{mX} = m_X \cdot V^{-1}$	$kg \cdot m^{-3}$	
mitochondrial concentration	C_{mtE}	$C_{mtE} = mtE \cdot V^{-1}$	$mtEU \cdot m^{-3}$	3
specific mitochondrial density	D_{mtE}	$D_{mtE} = mtE \cdot m_X^{-1}$	$mtEU \cdot kg^{-1}$	4
mitochondrial content, mtE per object X	mtE_X	$mtE_X = mtE \cdot N_X^{-1}$	$mtEU \cdot x^{-1}$	5
O₂ flow and flux				
flow, system	I_{O_2}	internal flow	$mol \cdot s^{-1}$	6
volume-specific flux	J_{V,O_2}	$J_{V,O_2} = I_{O_2} \cdot V^{-1}$	$mol \cdot s^{-1} \cdot m^{-3}$	7
flow per object X	$I_{O_2/X}$	$I_{O_2/X} = J_{V,O_2} \cdot C_{NX}^{-1}$	$mol \cdot s^{-1} \cdot x^{-1}$	8
mass-specific flux	$J_{O_2/mX}$	$J_{O_2/mX} = J_{V,O_2} \cdot C_{mX}^{-1}$	$mol \cdot s^{-1} \cdot kg^{-1}$	9
mitochondria-specific flux	$J_{O_2/mtE}$	$J_{O_2/mtE} = J_{V,O_2} \cdot C_{mtE}^{-1}$	$mol \cdot s^{-1} \cdot mtEU^{-1}$	10

- 993 1 The SI prefix k is used for the SI base unit of mass (kg = 1,000 g). In praxis, various SI prefixes are
 994 used for convenience, to make numbers easily readable, e.g., 1 mg tissue, cell or mitochondrial mass
 995 instead of 0.000001 kg.
- 996 2 In case sample $X =$ cells, the object number concentration is $C_{N_{cell}} = N_{cell} \cdot V^{-1}$, and volume may be
 997 expressed in [$dm^3 \equiv L$] or [$cm^3 = mL$]. See **Table 5** for different object types.
- 998 3 mt-concentration is an experimental variable, dependent on sample concentration: (1) $C_{mtE} = mtE \cdot V^{-1}$;
 999 (2) $C_{mtE} = mtE_X \cdot C_{NX}$; (3) $C_{mtE} = C_{mX} \cdot D_{mtE}$.
- 1000 4 If the amount of mitochondria, mtE , is expressed as mitochondrial mass, then D_{mtE} is the mass
 1001 fraction of mitochondria in the sample. If mtE is expressed as mitochondrial volume, V_{mt} , and the
 1002 mass of sample, m_X , is replaced by volume of sample, V_X , then D_{mtE} is the volume fraction of
 1003 mitochondria in the sample.
- 1004 5 $mtE_X = mtE \cdot N_X^{-1} = C_{mtE} \cdot C_{NX}^{-1}$.
- 1005 6 O₂ can be replaced by other chemicals B to study different reactions, e.g., ATP, H₂O₂, or
 1006 compartmental translocations, e.g., Ca²⁺.
- 1007 7 I_{O_2} and V are defined per instrument chamber as a system of constant volume (and constant
 1008 temperature), which may be closed or open. I_{O_2} is abbreviated for I_{r,O_2} , i.e., the metabolic or internal
 1009 O₂ flow of the chemical reaction r in which O₂ is consumed, hence the negative stoichiometric
 1010 number, $\nu_{O_2} = -1$. $I_{r,O_2} = d_r n_{O_2} / dt \cdot \nu_{O_2}^{-1}$. If r includes all chemical reactions in which O₂ participates, then
 1011 $d_r n_{O_2} = dn_{O_2} - d_e n_{O_2}$, where dn_{O_2} is the change in the amount of O₂ in the instrument chamber and $d_e n_{O_2}$
 1012 is the amount of O₂ added externally to the system. At steady state, by definition $dn_{O_2} = 0$, hence $d_r n_{O_2}$
 1013 $= -d_e n_{O_2}$.

- 1014 8 J_{V,O_2} is an experimental variable, expressed per volume of the instrument chamber.
 1015 9 $I_{O_2/X}$ is a physiological variable, depending on the size of entity X .
 1016 10 There are many ways to normalize for a mitochondrial marker, that are used in different experimental
 1017 approaches: (1) $J_{O_2/mtE} = J_{V,O_2} \cdot C_{mtE}^{-1}$; (2) $J_{O_2/mtE} = J_{V,O_2} \cdot C_{mX}^{-1} \cdot D_{mtE}^{-1} = J_{O_2/mX} \cdot D_{mtE}^{-1}$; (3) $J_{O_2/mtE} =$
 1018 $J_{V,O_2} \cdot C_{NX}^{-1} \cdot mtE_X^{-1} = I_{O_2/X} \cdot mtE_X^{-1}$; (4) $J_{O_2/mtE} = I_{O_2} \cdot mtE^{-1}$. The mt-elemental unit [mtEU] varies between
 1019 different mt-markers.
 1020
 1021

Table 5. Sample types, X, abbreviations, and quantification.

Identity of sample	X	N_X	Mass ^a	Volume	mt-Marker
mitochondrial preparation	mt-prep	[x]	[kg]	[m ³]	[mtEU]
isolated mitochondria	imt		m_{mt}	V_{mt}	mtE
tissue homogenate	thom		m_{thom}		mtE_{thom}
permeabilized tissue	pti		m_{pti}		mtE_{pti}
permeabilized fibre	pfi		m_{pfi}		mtE_{pfi}
permeabilized cell	pce	N_{pce}	M_{pce}	V_{pce}	mtE_{pce}
cells ^b	cell	N_{cell}	M_{cell}	V_{cell}	mtE_{cell}
intact cell, viable cell	vce	N_{vce}	M_{vce}	V_{vce}	
dead cell	dce	N_{dce}	M_{dce}	V_{dce}	
organism	org	N_{org}	M_{org}	V_{org}	

^a Instead of mass, the wet weight or dry weight is frequently stated, W_w or W_d .
 m_X is mass of the sample [kg], M_X is mass of the object [kg·x⁻¹].

^b Total cell count, $N_{cell} = N_{vce} + N_{dce}$

Cellular O₂ flow can be compared between cells of identical size. To take into account changes and differences in cell size, normalization is required to obtain cell size-specific or mitochondrial marker-specific O₂ flux (Renner *et al.* 2003).

The complexity changes when the sample is a whole organism studied as an experimental model. The scaling law in respiratory physiology reveals a strong interaction of O₂ flow and individual body mass of an organism, since *basal* metabolic rate (flow) does not increase linearly with body mass, whereas *maximum* mass-specific O₂ flux, \dot{V}_{O_2max} or \dot{V}_{O_2peak} , is approximately constant across a large range of individual body mass (Weibel and Hoppeler 2005), with individuals, breeds, and species deviating substantially from this relationship. \dot{V}_{O_2peak} of human endurance athletes is 60 to 80 mL O₂·min⁻¹·kg⁻¹ body mass, converted to $J_{O_2peak/M}$ of 45 to 60 nmol·s⁻¹·g⁻¹ (Gnaiger 2014; **Table 6**).

3.4. Normalization for mitochondrial content

Tissues can contain multiple cell populations that may have distinct mitochondrial subtypes. Mitochondria undergo dynamic fission and fusion cycles, and can exist in multiple stages and sizes that may be altered by a range of factors. The isolation of mitochondria (often achieved through differential centrifugation) can therefore yield a subsample of the mitochondrial types present in a tissue, depending on the isolation protocols utilized (*e.g.*, centrifugation speed). This possible bias should be taken into account when planning experiments using isolated mitochondria. Different sizes of mitochondria are enriched at specific centrifugation speeds, which can be used strategically for isolation of mitochondrial subpopulations.

Flow, Performance	=	Element function	x	Element density	x	Size of object
$\frac{\text{mol}\cdot\text{s}^{-1}}{x}$	=	$\frac{\text{mol}\cdot\text{s}^{-1}}{x_{mtE}}$	·	$\frac{x_{mtE}}{\text{kg}}$	·	$\frac{\text{kg}}{x}$

A

Flow	=	mt-specific flux	x	mt-structure, functional elements
$I_{O_2/X}$	=	$J_{O_2/mtE}$	·	mtE_X
				$\frac{mtE_X}{M_X} \cdot M_X$

B

$I_{O_2/X}$	=	$J_{O_2/mtE}$	·	D_{mtE}	·	M_X
$\frac{I_{O_2/X}}{M_X}$	=	$\frac{I_{O_2/X}}{mtE_X}$	·	$\frac{mtE_X}{M_X}$		
$I_{O_2/X}$	=	$J_{O_2/MX}$	·	M_X		
Flow	=	Object mass-specific flux	x	Mass of object		

Fig. 7. Structure-function analysis of performance of an organism, organ or tissue, or a cell (sample entity, X). O₂ flow, I_{O₂/X}, is the product of performance per functional element (element function, mitochondria-specific flux), element density (mitochondrial density, D_{mtE}), and size of entity X (mass, M_X). (A) Structured analysis: performance is the product of mitochondrial function (mt-specific flux) and structure (functional elements; D_{mtE} times mass of X). (B) Unstructured analysis: performance is the product of entity mass-specific flux, J_{O₂/MX} = I_{O₂/X}/M_X = I_{O₂/mX} [mol·s⁻¹·kg⁻¹] and size of entity, expressed as mass of X; M_X = m_X·N_X⁻¹ [kg·x⁻¹]. See Table 4 for further explanation of quantities and units. Modified from Gnaiger (2014).

Part of the mitochondrial content of a tissue is lost during preparation of isolated mitochondria. The fraction of isolated mitochondria obtained from a tissue sample is expressed as mitochondrial recovery. At a high mitochondrial recovery the fraction of isolated mitochondria is more representative of the total mitochondrial population than in preparations characterized by low recovery. Determination of the mitochondrial recovery and yield is based on measurement of the concentration of a mitochondrial marker in the stock of isolated mitochondria, C_{mtE,stock}, and crude tissue homogenate, C_{mtE,thom}, which simultaneously provides information on the specific mitochondrial density in the sample, D_{mtE} (Table 4).

Normalization is a problematic subject; it is essential to consider the question of the study. If the study aims at comparing tissue performance—such as the effects of a treatment on a specific tissue, then normalization for tissue mass or protein content is appropriate. However, if the aim is to find differences on mitochondrial function independent of mitochondrial density (Table 4), then normalization to a mitochondrial marker is imperative (Fig. 7). One cannot assume that quantitative changes in various markers—such as mitochondrial proteins—necessarily occur in parallel with one another. It should be established that the marker chosen is not selectively altered by the performed treatment. In conclusion, the normalization must reflect the question under investigation to reach a satisfying answer. On the other hand, the goal of comparing results across projects and institutions requires standardization on normalization for entry into a databank.

Mitochondrial concentration, C_{mtE}, and mitochondrial markers: Mitochondrial organelles comprise a dynamic cellular reticulum in various states of fusion and fission. Hence, the definition of an "amount" of mitochondria is often misconceived: mitochondria cannot be

1082 counted reliably as a number of occurring elements. Therefore, quantification of the "amount"
 1083 of mitochondria depends on the measurement of chosen mitochondrial markers. 'Mitochondria
 1084 are the structural and functional elemental units of cell respiration' (Gnaiger 2014). The
 1085 quantity of a mitochondrial marker can reflect the amount of *mitochondrial elements*, mtE ,
 1086 expressed in various mitochondrial elemental units [mtEU] specific for each measured mt-
 1087 marker (Table 4). However, since mitochondrial quality may change in response to stimuli—
 1088 particularly in mitochondrial dysfunction and after exercise training (Pesta *et al.* 2011; Campos
 1089 *et al.* 2017)—some markers can vary while others are unchanged: (1) Mitochondrial volume
 1090 and membrane area are structural markers, whereas mitochondrial protein mass is frequently
 1091 used as a marker for isolated mitochondria. (2) Molecular and enzymatic mitochondrial markers
 1092 (amounts or activities) can be selected as matrix markers, *e.g.*, citrate synthase activity, mtDNA;
 1093 mtIM-markers, *e.g.*, cytochrome *c* oxidase activity, aa_3 content, cardiolipin, or mtOM-markers,
 1094 *e.g.*, TOM20. (3) Extending the measurement of mitochondrial marker enzyme activity to
 1095 mitochondrial pathway capacity, ET- or OXPHOS-capacity can be considered as an integrative
 1096 functional mitochondrial marker.

1097 Depending on the type of mitochondrial marker, the mitochondrial elements, mtE , are
 1098 expressed in marker-specific units. Mitochondrial concentration in the measurement chamber
 1099 and the tissue of origin are quantified as (1) a quantity for normalization in functional analyses,
 1100 C_{mtE} , and (2) a physiological output that is the result of mitochondrial biogenesis and
 1101 degradation, D_{mtE} , respectively (Table 4). It is recommended, therefore, to distinguish
 1102 *experimental mitochondrial concentration*, $C_{mtE} = mtE/V$ and *physiological mitochondrial*
 1103 *density*, $D_{mtE} = mtE/m_X$. Then mitochondrial density is the amount of mitochondrial elements
 1104 per mass of tissue, which is a biological variable (Fig. 7). The experimental variable is
 1105 mitochondrial density multiplied by sample mass concentration in the measuring chamber, C_{mtE}
 1106 $= D_{mtE} \cdot C_{mX}$, or mitochondrial content multiplied by sample number concentration, $C_{mtE} =$
 1107 $mtE_X \cdot C_{NX}$ (Table 4).

1108 **Mitochondria-specific flux, $J_{O_2/mtE}$:** Volume-specific metabolic O_2 flux depends on: (1)
 1109 the sample concentration in the volume of the instrument chamber, C_{mX} , or C_{NX} ; (2) the
 1110 mitochondrial density in the sample, $D_{mtE} = mtE/m_X$ or $mtE_X = mtE/N_X$; and (3) the specific
 1111 mitochondrial activity or performance per elemental mitochondrial unit, $J_{O_2/mtE} = J_{V,O_2}/C_{mtE}$
 1112 [mol·s⁻¹·mtEU⁻¹] (Table 4). Obviously, the numerical results for $J_{O_2/mtE}$ vary with the type of
 1113 mitochondrial marker chosen for measurement of mtE and $C_{mtE} = mtE/V$ [mtEU·m⁻³].

1114 3.5. Evaluation of mitochondrial markers

1115 Different methods are implicated in the quantification of mitochondrial markers and have
 1116 different strengths. Some problems are common for all mitochondrial markers, mtE : (1)
 1117 Accuracy of measurement is crucial, since even a highly accurate and reproducible
 1118 measurement of O_2 flux results in an inaccurate and noisy expression if normalized by a biased
 1119 and noisy measurement of a mitochondrial marker. This problem is acute in mitochondrial
 1120 respiration because the denominators used (the mitochondrial markers) are often small moieties
 1121 of which accurate and precise determination is difficult. This problem can be avoided when O_2
 1122 fluxes measured in substrate-uncoupler-inhibitor titration protocols are normalized for flux in
 1123 a defined respiratory reference state, which is used as an *internal* marker and yields flux control
 1124 ratios, *FCRs*. *FCRs* are independent of *externally* measured markers and, therefore, are
 1125 statistically robust, considering the limitations of ratios in general (Jasienski and Bazzaz 1999).
 1126 *FCRs* indicate qualitative changes of mitochondrial respiratory control, with highest
 1127 quantitative resolution, separating the effect of mitochondrial density or concentration on $J_{O_2/mX}$
 1128 and $I_{O_2/X}$ from that of function per elemental mitochondrial marker, $J_{O_2/mtE}$ (Pesta *et al.* 2011;
 1129 Gnaiger 2014). (2) If mitochondrial quality does not change and only the amount of
 1130 mitochondria varies as a determinant of mass-specific flux, any marker is equally qualified in
 1132

1133 principle; then in practice selection of the optimum marker depends only on the accuracy and
 1134 precision of measurement of the mitochondrial marker. (3) If mitochondrial flux control ratios
 1135 change, then there may not be any best mitochondrial marker. In general, measurement of
 1136 multiple mitochondrial markers enables a comparison and evaluation of normalization for a
 1137 variety of mitochondrial markers. Particularly during postnatal development, the activity of
 1138 marker enzymes—such as cytochrome *c* oxidase and citrate synthase—follows different time
 1139 courses (Drahota *et al.* 2004). Evaluation of mitochondrial markers in healthy controls is
 1140 insufficient for providing guidelines for application in the diagnosis of pathological states and
 1141 specific treatments.

1142 In line with the concept of the respiratory control ratio (Chance and Williams 1955a), the
 1143 most readily used normalization is that of flux control ratios and flux control factors (Gnaiger
 1144 2014). Selection of the state of maximum flux in a protocol as the reference state has the
 1145 advantages of: (1) internal normalization; (2) statistical linearization of the response in the range
 1146 of 0 to 1; and (3) consideration of maximum flux for integrating a large number of elemental
 1147 steps in the OXPHOS- or ET-pathways. This reduces the risk of selecting a functional marker
 1148 that is specifically altered by the treatment or pathology, yet increases the chance that the highly
 1149 integrative pathway is disproportionately affected, *e.g.*, the OXPHOS- rather than ET-pathway
 1150 in case of an enzymatic defect in the phosphorylation-pathway. In this case, additional
 1151 information can be obtained by reporting flux control ratios based on a reference state which
 1152 indicates stable tissue-mass specific flux. Stereological determination of mitochondrial content
 1153 via two-dimensional transmission electron microscopy can have limitations due to the dynamics
 1154 of mitochondrial size (Meinild Lundby *et al.* 2017). Accurate determination of three-
 1155 dimensional volume by two-dimensional microscopy can be both time consuming and
 1156 statistically challenging (Larsen *et al.* 2012).

1157 The validity of using mitochondrial marker enzymes (citrate synthase activity, Complex
 1158 I–IV amount or activity) for normalization of flux is limited in part by the same factors that
 1159 apply to flux control ratios. Strong correlations between various mitochondrial markers and
 1160 citrate synthase activity (Reichmann *et al.* 1985; Boushel *et al.* 2007; Mogensen *et al.* 2007)
 1161 are expected in a specific tissue of healthy subjects and in disease states not specifically
 1162 targeting citrate synthase. Citrate synthase activity is acutely modifiable by exercise
 1163 (Tonkonogi *et al.* 1997; Leek *et al.* 2001). Evaluation of mitochondrial markers related to a
 1164 selected age and sex cohort cannot be extrapolated to provide recommendations for
 1165 normalization in respirometric diagnosis of disease, in different states of development and
 1166 ageing, different cell types, tissues, and species. mtDNA normalized to nDNA via qPCR is
 1167 correlated to functional mitochondrial markers including OXPHOS- and ET-capacity in some
 1168 cases (Puntschart *et al.* 1995; Wang *et al.* 1999; Menshikova *et al.* 2006; Boushel *et al.* 2007),
 1169 but lack of such correlations have been reported (Menshikova *et al.* 2005; Schultz and Wiesner
 1170 2000; Pesta *et al.* 2011). Several studies indicate a strong correlation between cardiolipin
 1171 content and increase in mitochondrial function with exercise (Menshikova *et al.* 2005;
 1172 Menshikova *et al.* 2007; Larsen *et al.* 2012; Faber *et al.* 2014), but it has not been evaluated as
 1173 a general mitochondrial biomarker in disease.

1174

1175 3.6. Conversion: units

1176

1177 Many different units have been used to report the O₂ consumption rate, OCR (**Table 6**).
 1178 *SI* base units provide the common reference to introduce the theoretical principles (**Fig. 6**), and
 1179 are used with appropriately chosen *SI* prefixes to express numerical data in the most practical
 1180 format, with an effort towards unification within specific areas of application (**Table 7**).
 1181 Reporting data in *SI* units—including the mole [mol], coulomb [C], joule [J], and second [s]—
 1182 should be encouraged, particularly by journals which propose the use of *SI* units.

1183

1184
1185
1186
1187

Table 6. Conversion of various units used in respirometry and ergometry. e^- is the number of electrons or reducing equivalents. z_B is the charge number of entity B.

1 Unit	x	Multiplication factor	SI-unit	Note
ng.atom O \cdot s $^{-1}$	(2 e^-)	0.5	nmol O $_2$ \cdot s $^{-1}$	
ng.atom O \cdot min $^{-1}$	(2 e^-)	8.33	pmol O $_2$ \cdot s $^{-1}$	
natom O \cdot min $^{-1}$	(2 e^-)	8.33	pmol O $_2$ \cdot s $^{-1}$	
nmol O $_2$ \cdot min $^{-1}$	(4 e^-)	16.67	pmol O $_2$ \cdot s $^{-1}$	
nmol O $_2$ \cdot h $^{-1}$	(4 e^-)	0.2778	pmol O $_2$ \cdot s $^{-1}$	
mL O $_2$ \cdot min $^{-1}$ at STPD ^a		0.744	μ mol O $_2$ \cdot s $^{-1}$	1
W = J/s at -470 kJ/mol O $_2$		-2.128	μ mol O $_2$ \cdot s $^{-1}$	
mA = mC \cdot s $^{-1}$	($z_{H^+} = 1$)	10.36	nmol H $^+$ \cdot s $^{-1}$	2
mA = mC \cdot s $^{-1}$	($z_{O_2} = 4$)	2.59	nmol O $_2$ \cdot s $^{-1}$	2
nmol H $^+$ \cdot s $^{-1}$	($z_{H^+} = 1$)	0.09649	mA	3
nmol O $_2$ \cdot s $^{-1}$	($z_{O_2} = 4$)	0.38594	mA	3

1188
1189
1190
1191
1192
1193
1194
1195

- 1 At standard temperature and pressure dry (STPD: 0 °C = 273.15 K and 1 atm = 101.325 kPa = 760 mmHg), the molar volume of an ideal gas, V_m , and V_{m,O_2} is 22.414 and 22.392 L \cdot mol $^{-1}$, respectively. Rounded to three decimal places, both values yield the conversion factor of 0.744. For comparison at NTPD (20 °C), V_{m,O_2} is 24.038 L \cdot mol $^{-1}$. Note that the *SI* standard pressure is 100 kPa.
- 2 The multiplication factor is $10^6/(z_B \cdot F)$.
- 3 The multiplication factor is $z_B \cdot F/10^6$.

1196
1197
1198
1199
1200
1201
1202
1203
1204
1205

Although volume is expressed as m 3 using the *SI* base unit, the litre [dm 3] is a conventional unit of volume for concentration and is used for most solution chemical kinetics. If one multiplies $I_{O_2/cell}$ by C_{Ncell} , then the result will not only be the amount of O $_2$ [mol] consumed per time [s $^{-1}$] in one litre [L $^{-1}$], but also the change in O $_2$ concentration per second (for any volume of an ideally closed system). This is ideal for kinetic modeling as it blends with chemical rate equations where concentrations are typically expressed in mol \cdot L $^{-1}$ (Wagner *et al.* 2011). In studies of multinuclear cells—such as differentiated skeletal muscle cells—it is easy to determine the number of nuclei but not the total number of cells. A generalized concept, therefore, is obtained by substituting cells by nuclei as the sample entity. This does not hold, however, for enucleated platelets.

1206
1207
1208
1209
1210
1211
1212
1213
1214
1215
1216
1217
1218
1219
1220

For studies of cells, we recommend that respiration be expressed, as far as possible, as: (1) O $_2$ flux normalized for a mitochondrial marker, for separation of the effects of mitochondrial quality and content on cell respiration (this includes *FCRs* as a normalization for a functional mitochondrial marker); (2) O $_2$ flux in units of cell volume or mass, for comparison of respiration of cells with different cell size (Renner *et al.* 2003) and with studies on tissue preparations, and (3) O $_2$ flow in units of attomole (10^{-18} mol) of O $_2$ consumed in a second by each cell [amol \cdot s $^{-1}$ \cdot cell $^{-1}$], numerically equivalent to [pmol \cdot s $^{-1}$ \cdot 10 $^{-6}$ cells]. This convention allows information to be easily used when designing experiments in which O $_2$ flow must be considered. For example, to estimate the volume-specific O $_2$ flux in an instrument chamber that would be expected at a particular cell number concentration, one simply needs to multiply the flow per cell by the number of cells per volume of interest. This provides the amount of O $_2$ [mol] consumed per time [s $^{-1}$] per unit volume [L $^{-1}$]. At an O $_2$ flow of 100 amol \cdot s $^{-1}$ \cdot cell $^{-1}$ and a cell density of 10 9 cells \cdot L $^{-1}$ (10 6 cells \cdot mL $^{-1}$), the volume-specific O $_2$ flux is 100 nmol \cdot s $^{-1}$ \cdot L $^{-1}$ (100 pmol \cdot s $^{-1}$ \cdot mL $^{-1}$).

1221

Table 7. Conversion of units with preservation of numerical values.

Name	Frequently used unit	Equivalent unit	Note
volume-specific flux, J_{V,O_2}	$\text{pmol}\cdot\text{s}^{-1}\cdot\text{mL}^{-1}$ $\text{mmol}\cdot\text{s}^{-1}\cdot\text{L}^{-1}$	$\text{nmol}\cdot\text{s}^{-1}\cdot\text{L}^{-1}$ $\text{mol}\cdot\text{s}^{-1}\cdot\text{m}^{-3}$	1
cell-specific flow, $I_{O_2/\text{cell}}$	$\text{pmol}\cdot\text{s}^{-1}\cdot 10^{-6}$ cells	$\text{amol}\cdot\text{s}^{-1}\cdot\text{cell}^{-1}$	2
	$\text{pmol}\cdot\text{s}^{-1}\cdot 10^{-9}$ cells	$\text{zmol}\cdot\text{s}^{-1}\cdot\text{cell}^{-1}$	3
cell number concentration, C_{Nce}	10^6 cells $\cdot\text{mL}^{-1}$	10^9 cells $\cdot\text{L}^{-1}$	
mitochondrial protein concentration, C_{mtE}	0.1 mg $\cdot\text{mL}^{-1}$	0.1 g $\cdot\text{L}^{-1}$	
mass-specific flux, $J_{O_2/m}$	$\text{pmol}\cdot\text{s}^{-1}\cdot\text{mg}^{-1}$	$\text{nmol}\cdot\text{s}^{-1}\cdot\text{g}^{-1}$	4
catabolic power, P_k	$\mu\text{W}\cdot 10^{-6}$ cells	$\text{pW}\cdot\text{cell}^{-1}$	1
Volume	1,000 L	m^3 (1,000 kg)	
	L	dm^3 (kg)	
	mL	cm^3 (g)	
	μL	mm^3 (mg)	
	fL	μm^3 (pg)	5
amount of substance concentration	$\text{M} = \text{mol}\cdot\text{L}^{-1}$	$\text{mol}\cdot\text{dm}^{-3}$	

1222

1223 1 pmol: picomole = 10^{-12} mol1224 2 amol: attomole = 10^{-18} mol1225 3 zmol: zeptomole = 10^{-21} mol

1226

1227 ET-capacity in human cell types including HEK 293, primary HUVEC and fibroblasts
 1228 ranges from 50 to 180 $\text{amol}\cdot\text{s}^{-1}\cdot\text{cell}^{-1}$, measured in intact cells in the noncoupled state (see
 1229 Gnaiger 2014). At 100 $\text{amol}\cdot\text{s}^{-1}\cdot\text{cell}^{-1}$ corrected for *Rox*, the current across the mt-membranes,
 1230 I_{H^+e} , approximates 193 $\text{pA}\cdot\text{cell}^{-1}$ or 0.2 nA per cell. See Rich (2003) for an extension of
 1231 quantitative bioenergetics from the molecular to the human scale, with a transmembrane proton
 1232 flux equivalent to 520 A in an adult at a catabolic power of -110 W. Modelling approaches
 1233 illustrate the link between protonmotive force and currents (Willis *et al.* 2016).

1234 We consider isolated mitochondria as powerhouses and proton pumps as molecular
 1235 machines to relate experimental results to energy metabolism of the intact cell. The cellular
 1236 P_{\gg}/O_2 based on oxidation of glycogen is increased by the glycolytic (fermentative) substrate-
 1237 level phosphorylation of 3 P_{\gg}/Glyc or 0.5 mol P_{\gg} for each mol O_2 consumed in the complete
 1238 oxidation of a mol glycosyl unit (Glyc). Adding 0.5 to the mitochondrial P_{\gg}/O_2 ratio of 5.4
 1239 yields a bioenergetic cell physiological P_{\gg}/O_2 ratio close to 6. Two NADH equivalents are
 1240 formed during glycolysis and transported from the cytosol into the mitochondrial matrix, either
 1241 by the malate-aspartate shuttle or by the glycerophosphate shuttle (Fig. 1) resulting in different
 1242 theoretical yields of ATP generated by mitochondria, the energetic cost of which potentially
 1243 must be taken into account. Considering also substrate-level phosphorylation in the TCA cycle,
 1244 this high P_{\gg}/O_2 ratio not only reflects proton translocation and OXPHOS studied in isolation,
 1245 but integrates mitochondrial physiology with energy transformation in the living cell (Gnaiger
 1246 1993a).

1247

1248

1249 **4. Conclusions**

1250

1251 MitoEAGLE can serve as a gateway to better diagnose mitochondrial respiratory defects
 1252 linked to genetic variation, age-related health risks, sex-specific mitochondrial performance,
 1253 lifestyle with its effects on degenerative diseases, and thermal and chemical environment. The
 1254 present recommendations on coupling control states and rates, linked to the concept of the

1255 protonmotive force, are focused on studies with mitochondrial preparations. These will be
 1256 extended in a series of reports on pathway control of mitochondrial respiration, respiratory
 1257 states in intact cells, and harmonization of experimental procedures.
 1258

1259 **Box 3: Mitochondrial and cell respiration**

1260
 1261 Mitochondrial and cell respiration is the process of exergonic and exothermic energy
 1262 transformation in which scalar redox reactions are coupled to vectorial ion translocation across
 1263 a semipermeable membrane, which separates the small volume of a bacterial cell or
 1264 mitochondrion from the larger volume of its surroundings. The electrochemical exergy can be
 1265 partially conserved in the phosphorylation of ADP to ATP or in ion pumping, or dissipated in
 1266 an electrochemical short-circuit. Respiration is thus clearly distinguished from fermentation as
 1267 the counterpart of cellular core energy metabolism (**Fig. 1**). Respiration is separated in
 1268 mitochondrial preparations from the partial contribution of fermentative pathways of the intact
 1269 cell. Residual O₂ consumption—as measured after inhibition of mitochondrial electron
 1270 transfer—does not belong to the class of catabolic reactions coupled to the phosphorylation of
 1271 ADP to ATP and is, therefore, subtracted from total O₂ consumption to obtain baseline-
 1272 corrected respiration.

1273 Mitochondrial dysfunction is associated with a wide variety of genetic and degenerative
 1274 diseases. Robust mitochondrial function is supported by physical exercise and caloric balance,
 1275 and is central for sustained metabolic health throughout life. Therefore, a consistent
 1276 presentation of mitochondrial physiology will improve our understanding of the etiology of
 1277 disease and the diagnostic repertoire of mitochondrial medicine, with a focus on protective
 1278 medicine, lifestyle and healthy aging.
 1279

1280
 1281 The optimal choice for expressing mitochondrial and cell respiration (**Box 3**) as O₂ flow
 1282 per biological sample, and normalization for specific tissue-markers (volume, mass, protein)
 1283 and mitochondrial markers (volume, protein, content, mtDNA, activity of marker enzymes,
 1284 respiratory reference state) is guided by the scientific question under study. Interpretation of
 1285 the data depends critically on appropriate normalization.

1286 We recommend for studies with mitochondrial preparations:

- 1287 • Normalization of respiratory rates should be provided as far as possible: (1) biophysical
 1288 normalization: on a per cell basis as O₂ flow (may not be possible when dealing with
 1289 tissues); (2) cellular normalization: per g cell or tissue protein, or per cell or tissue mass
 1290 as mass-specific O₂ flux; and (3) mitochondrial normalization: per mitochondrial marker
 1291 as mt-specific flux. With information on cell size and the use of multiple normalizations,
 1292 maximum potential information is available (Renner *et al.* 2003; Wagner *et al.* 2011;
 1293 Gnaiger 2014). Reporting flow in a respiratory chamber [nmol·s⁻¹] is discouraged, since
 1294 it restricts the analysis to intra-experimental comparison of relative (qualitative)
 1295 differences.
- 1296 • Catabolic mitochondrial respiration is distinguished from residual oxygen consumption.
 1297 Fluxes in mitochondrial coupling states should be, as far as possible, corrected for residual
 1298 oxygen consumption.
- 1299 • In studies of isolated mitochondria, the mitochondrial recovery and yield should be
 1300 reported. Experimental criteria for evaluation of purity versus integrity should be
 1301 considered. Mitochondrial markers—such as citrate synthase activity as an enzymatic
 1302 matrix marker—provide a link to the tissue of origin on the basis of calculating the
 1303 mitochondrial recovery, *i.e.*, the fraction of mitochondrial marker obtained from a unit
 1304 mass of tissue. Total mitochondrial protein is frequently applied as a mitochondrial
 1305 marker, which is restricted to isolated mitochondria.

- 1306 • In studies of permeabilized cells, the viability of the cell culture or cell suspension of
 1307 origin should be reported. Normalization should be evaluated for total cell count or viable
 1308 cell count.
- 1309 • Terms and symbols are summarized in **Table 8**. Their use will facilitate transdisciplinary
 1310 communication and support further developments towards a consistent theory of
 1311 bioenergetics and mitochondrial physiology.
- 1312 • Technical terms related to and defined with normal words can be used as index terms in
 1313 databases, support the creation of ontologies towards semantic information processing
 1314 (MitoPedia), and help in communicating analytical findings as impactful data-driven
 1315 stories. ‘*Making data available without making it understandable may be worse than not*
 1316 *making it available at all*’ (National Academies of Sciences, Engineering, and Medicine
 1317 2018). This is a call to carefully contribute to FAIR principles (Findable, Accessible,
 1318 Interoperable, Reusable) for the sharing of scientific data.

1320 **Table 8. Terms, symbols, and units.**

Term	Symbol	Unit	Links and comments
1326 alternative quinol oxidase	AOX		Fig. 2A
1327 amount of substance B	n_B	[mol]	
1328 cell number	N_{cell}	[x]	Tab. 5; $N_{\text{cell}} = N_{\text{vce}} + N_{\text{dce}}$
1329 cell viability index	CVI		$CVI = N_{\text{vce}}/N_{\text{cell}} = 1 - N_{\text{dce}}/N_{\text{cell}}$
1330 Complexes I to IV	CI to CIV		respiratory ET Complexes; Fig. 2A
1331 concentration of substance B	$c_B = n_B \cdot V^{-1}$; [B]	[mol·m ⁻³]	Box 2
1332 dead cell number	N_{dce}	[x]	Tab. 5; non-viable cells, loss of plasma membrane barrier function
1334 electron transfer system	ETS		Fig. 2A, Fig. 4
1335 flow, for substance B	I_B	[mol·s ⁻¹]	system-related extensive quantity; Fig. 6
1336 flux, for substance B	J_B	<i>varies</i>	size-specific quantity; Fig. 6
1337 inorganic phosphate	P_i		Fig. 2C
1338 intact cell number, viable cell number	N_{vce}	[x]	Tab. 5; viable cells, intact of plasma membrane barrier function
1340 LEAK	LEAK		Tab. 1, Fig. 4
1341 mass of sample X	m_X	[kg]	Tab. 4
1342 mass of entity X	M_X	[kg]	mass of object X; Tab. 4
1343 MITOCARTA			https://www.broadinstitute.org/scientific-community/science/programs/metabolic-disease-program/publications/mitocarta/mitocarta-in-0
1348 MitoPedia			http://www.bioblast.at/index.php/MitoPedia
1349 mitochondria or mitochondrial	mt		Box 1
1350 mitochondrial DNA	mtDNA		Box 1
1351 mitochondrial concentration	$C_{\text{mtE}} = \text{mtE} \cdot V^{-1}$	[mtEU·m ⁻³]	Tab. 4
1352 mitochondrial content	$\text{mtE}_X = \text{mtE} \cdot N_X^{-1}$	[mtEU·x ⁻¹]	Tab. 4
1353 mitochondrial elemental unit	mtEU	<i>varies</i>	Tab. 4, specific units for mt-marker
1354 mitochondrial inner membrane	mtIM		Fig. 1; MIM is widely used; the first M is replaced by mt; Box 1
1356 mitochondrial outer membrane	mtOM		Fig. 1; MOM is widely used; the first M is replaced by mt; Box 1
1358 mitochondrial recovery	Y_{mtE}		fraction of <i>mtE</i> recovered in sample from the tissue of origin
1360 mitochondrial yield	$Y_{\text{mtE}/m}$		$Y_{\text{mtE}/m} = Y_{\text{mtE}} \cdot D_{\text{mtE}}$
1361 negative	neg		Fig. 2C
1362 number concentration of X	C_{NX}	[x·m ⁻³]	Tab. 4
1363 number of entities X	N_X	[x]	Tab. 4, Fig. 7
1364 number of entity B	N_B	[x]	Tab. 4

1365	oxidative phosphorylation	OXPPOS		Tab. 1, Fig. 4
1366	oxygen concentration	$c_{O_2} = n_{O_2} \cdot V^{-1}$; $[O_2]$	$[\text{mol} \cdot \text{m}^{-3}]$	Section 3.2
1367	permeabilized cell number	N_{pce}	$[x]$	Tab. 5; experimental permeabilization of plasma membrane; $N_{pce} = N_{cell}$
1368				
1369	phosphorylation of ADP to ATP	P»		Section 2.2
1370	positive	pos		Fig. 2C
1371	proton in the negative compartment	H^{+}_{neg}		Fig. 2C
1372	proton in the positive compartment	H^{+}_{pos}		Fig. 2C
1373	rate of electron transfer in ET state	E		ET-capacity; Tab. 1
1374	rate of LEAK respiration	L		Tab. 1
1375	rate of oxidative phosphorylation	P		OXPPOS capacity; Tab. 1
1376	rate of residual oxygen consumption	ROx		Tab. 1
1377	residual oxygen consumption	ROX		Tab. 1
1378	respiratory supercomplex	SC I _n III _n IV _n		Box 1; supramolecular assemblies composed of variable copy numbers (n) of CI, CIII and CIV
1379				
1380				
1381	specific mitochondrial density	$D_{mtE} = mtE \cdot m_X^{-1}$	$[\text{mtEU} \cdot \text{kg}^{-1}]$	Tab. 4
1382	volume	V	$[\text{m}^{-3}]$	Tab. 7
1383	weight, dry weight	W_d	$[\text{kg}]$	used as mass of sample X; Fig. 6
1384	weight, wet weight	W_w	$[\text{kg}]$	used as mass of sample X; Fig. 6
1385				

1386

1387

1388 Acknowledgements

1389 We thank M. Beno for management assistance. Supported by COST Action CA15203
1390 MitoEAGLE and K-Regio project MitoFit (E.G.).

1391

1392 **Competing financial interests:** E.G. is founder and CEO of Oroboros Instruments, Innsbruck,
1393 Austria.

1394

1395

1396 5. References

1397

1398 Altmann R (1894) Die Elementarorganismen und ihre Beziehungen zu den Zellen. Zweite vermehrte Auflage.
1399 Verlag Von Veit & Comp, Leipzig:160 pp.

1400 Beard DA (2005) A biophysical model of the mitochondrial respiratory system and oxidative phosphorylation.
1401 PLoS Comput Biol 1(4):e36.

1402 Benda C (1898) Weitere Mitteilungen über die Mitochondria. Verh Dtsch Physiol Ges:376-83.

1403 Birkedal R, Laasmaa M, Vendelin M (2014) The location of energetic compartments affects energetic
1404 communication in cardiomyocytes. Front Physiol 5:376.

1405 Breton S, Beaupré HD, Stewart DT, Hoeh WR, Blier PU (2007) The unusual system of doubly uniparental
1406 inheritance of mtDNA: isn't one enough? Trends Genet 23:465-74.

1407 Brown GC (1992) Control of respiration and ATP synthesis in mammalian mitochondria and cells. Biochem J
1408 284:1-13.

1409 Calvo SE, Klauser CR, Mootha VK (2016) MitoCarta2.0: an updated inventory of mammalian mitochondrial
1410 proteins. Nucleic Acids Research 44:D1251-7.

1411 Calvo SE, Julien O, Clauser KR, Shen H, Kamer KJ, Wells JA, Mootha VK (2017) Comparative analysis of
1412 mitochondrial N-termini from mouse, human, and yeast. Mol Cell Proteomics 16:512-23.

1413 Campos JC, Queliconi BB, Bozi LHM, Bechara LRG, Dourado PMM, Andres AM, Jannig PR, Gomes KMS,
1414 Zambelli VO, Rocha-Resende C, Guatimosim S, Brum PC, Mochly-Rosen D, Gottlieb RA, Kowaltowski AJ,
1415 Ferreira JCB (2017) Exercise reestablishes autophagic flux and mitochondrial quality control in heart failure.
1416 Autophagy 13:1304-317.

1417 Canton M, Luvisetto S, Schmehl I, Azzone GF (1995) The nature of mitochondrial respiration and
1418 discrimination between membrane and pump properties. Biochem J 310:477-81.

1419 Chance B, Williams GR (1955a) Respiratory enzymes in oxidative phosphorylation. I. Kinetics of oxygen
1420 utilization. J Biol Chem 217:383-93.

1421 Chance B, Williams GR (1955b) Respiratory enzymes in oxidative phosphorylation: III. The steady state. J Biol
1422 Chem 217:409-27.

- 1423 Chance B, Williams GR (1955c) Respiratory enzymes in oxidative phosphorylation. IV. The respiratory chain. *J*
 1424 *Biol Chem* 217:429-38.
- 1425 Chance B, Williams GR (1956) The respiratory chain and oxidative phosphorylation. *Adv Enzymol Relat Subj*
 1426 *Biochem* 17:65-134.
- 1427 Cobb LJ, Lee C, Xiao J, Yen K, Wong RG, Nakamura HK, Mehta HH, Gao Q, Ashur C, Huffman DM, Wan J,
 1428 Muzumdar R, Barzilai N, Cohen P (2016) Naturally occurring mitochondrial-derived peptides are age-
 1429 dependent regulators of apoptosis, insulin sensitivity, and inflammatory markers. *Aging (Albany NY)* 8:796-
 1430 809.
- 1431 Cohen ER, Cvitas T, Frey JG, Holmström B, Kuchitsu K, Marquardt R, Mills I, Pavese F, Quack M, Stohner J,
 1432 Strauss HL, Takami M, Thor HL (2008) Quantities, units and symbols in physical chemistry, IUPAC Green
 1433 Book, 3rd Edition, 2nd Printing, IUPAC & RSC Publishing, Cambridge.
- 1434 Cooper H, Hedges LV, Valentine JC, eds (2009) The handbook of research synthesis and meta-analysis. Russell
 1435 Sage Foundation.
- 1436 Coopersmith J (2010) Energy, the subtle concept. The discovery of Feynman's blocks from Leibnitz to Einstein.
 1437 Oxford University Press:400 pp.
- 1438 Cummins J (1998) Mitochondrial DNA in mammalian reproduction. *Rev Reprod* 3:172-82.
- 1439 Dai Q, Shah AA, Garde RV, Yonish BA, Zhang L, Medvitz NA, Miller SE, Hansen EL, Dunn CN, Price TM
 1440 (2013) A truncated progesterone receptor (PR-M) localizes to the mitochondrion and controls cellular
 1441 respiration. *Mol Endocrinol* 27:741-53.
- 1442 Divakaruni AS, Brand MD (2011) The regulation and physiology of mitochondrial proton leak. *Physiology*
 1443 (Bethesda) 26:192-205.
- 1444 Doerrier C, Garcia-Souza LF, Krumschnabel G, Wohlfarter Y, Mészáros AT, Gnaiger E (2018) High-Resolution
 1445 FluoRespirometry and OXPHOS protocols for human cells, permeabilized fibres from small biopsies of
 1446 muscle and isolated mitochondria. *Methods Mol. Biol.* (in press)
- 1447 Doskey CM, van 't Erve TJ, Wagner BA, Buettner GR (2015) Moles of a substance per cell is a highly
 1448 informative dosing metric in cell culture. *PLOS ONE* 10:e0132572.
- 1449 Drahotová Z, Milerová M, Stieglerová A, Houstek J, Ostádal B (2004) Developmental changes of cytochrome *c*
 1450 oxidase and citrate synthase in rat heart homogenate. *Physiol Res* 53:119-22.
- 1451 Duarte FV, Palmeira CM, Rolo AP (2014) The role of microRNAs in mitochondria: small players acting wide.
 1452 *Genes (Basel)* 5:865-86.
- 1453 Ernster L, Schatz G (1981) Mitochondria: a historical review. *J Cell Biol* 91:227s-55s.
- 1454 Estabrook RW (1967) Mitochondrial respiratory control and the polarographic measurement of ADP:O ratios.
 1455 *Methods Enzymol* 10:41-7.
- 1456 Faber C, Zhu ZJ, Castellino S, Wagner DS, Brown RH, Peterson RA, Gates L, Barton J, Bickett M, Hagerty L,
 1457 Kimbrough C, Sola M, Bailey D, Jordan H, Elangbam CS (2014) Cardiolipin profiles as a potential
 1458 biomarker of mitochondrial health in diet-induced obese mice subjected to exercise, diet-restriction and
 1459 ephedrine treatment. *J Appl Toxicol* 34:1122-9.
- 1460 Fell D (1997) Understanding the control of metabolism. Portland Press.
- 1461 Garlid KD, Beavis AD, Ratkje SK (1989) On the nature of ion leaks in energy-transducing membranes. *Biochim*
 1462 *Biophys Acta* 976:109-20.
- 1463 Garlid KD, Semrad C, Zinchenko V. Does redox slip contribute significantly to mitochondrial respiration? In:
 1464 Schuster S, Rigoulet M, Ouhabi R, Mazat J-P, eds (1993) Modern trends in biothermokinetics. Plenum Press,
 1465 New York, London:287-93.
- 1466 Gerö D, Szabo C (2016) Glucocorticoids suppress mitochondrial oxidant production via upregulation of
 1467 uncoupling protein 2 in hyperglycemic endothelial cells. *PLoS One* 11:e0154813.
- 1468 Gnaiger E. Efficiency and power strategies under hypoxia. Is low efficiency at high glycolytic ATP production a
 1469 paradox? In: *Surviving Hypoxia: Mechanisms of Control and Adaptation*. Hochachka PW, Lutz PL, Sick T,
 1470 Rosenthal M, Van den Thillart G, eds (1993a) CRC Press, Boca Raton, Ann Arbor, London, Tokyo:77-109.
- 1471 Gnaiger E (1993b) Nonequilibrium thermodynamics of energy transformations. *Pure Appl Chem* 65:1983-2002.
- 1472 Gnaiger E (2001) Bioenergetics at low oxygen: dependence of respiration and phosphorylation on oxygen and
 1473 adenosine diphosphate supply. *Respir Physiol* 128:277-97.
- 1474 Gnaiger E (2009) Capacity of oxidative phosphorylation in human skeletal muscle. New perspectives of
 1475 mitochondrial physiology. *Int J Biochem Cell Biol* 41:1837-45.
- 1476 Gnaiger E (2014) Mitochondrial pathways and respiratory control. An introduction to OXPHOS analysis. 4th ed.
 1477 *Mitochondr Physiol Network* 19.12. Oroboros MiPNet Publications, Innsbruck:80 pp.
- 1478 Gnaiger E, Méndez G, Hand SC (2000) High phosphorylation efficiency and depression of uncoupled respiration
 1479 in mitochondria under hypoxia. *Proc Natl Acad Sci USA* 97:11080-5.
- 1480 Greggio C, Jha P, Kulkarni SS, Lagarrigue S, Broskey NT, Boutant M, Wang X, Conde Alonso S, Ofori E,
 1481 Auwerx J, Cantó C, Amati F (2017) Enhanced respiratory chain supercomplex formation in response to
 1482 exercise in human skeletal muscle. *Cell Metab* 25:301-11.
- 1483 Hinkle PC (2005) P/O ratios of mitochondrial oxidative phosphorylation. *Biochim Biophys Acta* 1706:1-11.

- 1484 Hofstadter DR (1979) Gödel, Escher, Bach: An eternal golden braid. A metaphorical fugue on minds and
 1485 machines in the spirit of Lewis Carroll. Harvester Press:499 pp.
- 1486 Illaste A, Laasmaa M, Peterson P, Vendelin M (2012) Analysis of molecular movement reveals latticelike
 1487 obstructions to diffusion in heart muscle cells. *Biophys J* 102:739-48.
- 1488 Jasienski M, Bazzaz FA (1999) The fallacy of ratios and the testability of models in biology. *Oikos* 84:321-26.
- 1489 Jepihhina N, Beraud N, Sepp M, Birkedal R, Vendelin M (2011) Permeabilized rat cardiomyocyte response
 1490 demonstrates intracellular origin of diffusion obstacles. *Biophys J* 101:2112-21.
- 1491 Klepinin A, Ounpuu L, Guzun R, Chekulayev V, Timohhina N, Tepp K, Shevchuk I, Schlattner U, Kaambre T
 1492 (2016) Simple oxygraphic analysis for the presence of adenylate kinase 1 and 2 in normal and tumor cells. *J*
 1493 *Bioenerg Biomembr* 48:531-48.
- 1494 Klingenberg M (2017) UCP1 - A sophisticated energy valve. *Biochimie* 134:19-27.
- 1495 Koit A, Shevchuk I, Ounpuu L, Klepinin A, Chekulayev V, Timohhina N, Tepp K, Puurand M, Truu L, Heck K,
 1496 Valvere V, Guzun R, Kaambre T (2017) Mitochondrial respiration in human colorectal and breast cancer
 1497 clinical material is regulated differently. *Oxid Med Cell Longev* 1372640.
- 1498 Komlódi T, Tretter L (2017) Methylene blue stimulates substrate-level phosphorylation catalysed by succinyl-
 1499 CoA ligase in the citric acid cycle. *Neuropharmacology* 123:287-98.
- 1500 Lane N (2005) Power, sex, suicide: mitochondria and the meaning of life. Oxford University Press:354 pp.
- 1501 Larsen S, Nielsen J, Neigaard Nielsen C, Nielsen LB, Wibrand F, Stride N, Schroder HD, Boushel RC, Helge
 1502 JW, Dela F, Hey-Mogensen M (2012) Biomarkers of mitochondrial content in skeletal muscle of healthy
 1503 young human subjects. *J Physiol* 590:3349-60.
- 1504 Lee C, Zeng J, Drew BG, Sallam T, Martin-Montalvo A, Wan J, Kim SJ, Mehta H, Hevener AL, de Cabo R,
 1505 Cohen P (2015) The mitochondrial-derived peptide MOTS-c promotes metabolic homeostasis and reduces
 1506 obesity and insulin resistance. *Cell Metab* 21:443-54.
- 1507 Lee SR, Kim HK, Song IS, Youm J, Dizon LA, Jeong SH, Ko TH, Heo HJ, Ko KS, Rhee BD, Kim N, Han J
 1508 (2013) Glucocorticoids and their receptors: insights into specific roles in mitochondria. *Prog Biophys Mol*
 1509 *Biol* 112:44-54.
- 1510 Leek BT, Mudaliar SR, Henry R, Mathieu-Costello O, Richardson RS (2001) Effect of acute exercise on citrate
 1511 synthase activity in untrained and trained human skeletal muscle. *Am J Physiol Regul Integr Comp Physiol*
 1512 280:R441-7.
- 1513 Lemieux H, Blier PU, Gnaiger E (2017) Remodeling pathway control of mitochondrial respiratory capacity by
 1514 temperature in mouse heart: electron flow through the Q-junction in permeabilized fibers. *Sci Rep* 7:2840.
- 1515 Lenaz G, Tioli G, Falasca AI, Genova ML (2017) Respiratory supercomplexes in mitochondria. In: Mechanisms
 1516 of primary energy trasduction in biology. M Wikstrom (ed) Royal Society of Chemistry Publishing, London,
 1517 UK:296-337.
- 1518 Margulis L (1970) Origin of eukaryotic cells. New Haven: Yale University Press.
- 1519 Meinild Lundby AK, Jacobs RA, Gehrig S, de Leur J, Hauser M, Bonne TC, Flück D, Dandanell S, Kirk N,
 1520 Kaech A, Ziegler U, Larsen S, Lundby C (2018) Exercise training increases skeletal muscle mitochondrial
 1521 volume density by enlargement of existing mitochondria and not de novo biogenesis. *Acta Physiol* 222,
 1522 e12905.
- 1523 Menshikova EV, Ritov VB, Fairfull L, Ferrell RE, Kelley DE, Goodpaster BH (2006) Effects of exercise on
 1524 mitochondrial content and function in aging human skeletal muscle. *J Gerontol A Biol Sci Med Sci* 61:534-
 1525 40.
- 1526 Menshikova EV, Ritov VB, Ferrell RE, Azuma K, Goodpaster BH, Kelley DE (2007) Characteristics of skeletal
 1527 muscle mitochondrial biogenesis induced by moderate-intensity exercise and weight loss in obesity. *J Appl*
 1528 *Physiol* (1985) 103:21-7.
- 1529 Menshikova EV, Ritov VB, Toledo FG, Ferrell RE, Goodpaster BH, Kelley DE (2005) Effects of weight loss
 1530 and physical activity on skeletal muscle mitochondrial function in obesity. *Am J Physiol Endocrinol Metab*
 1531 288:E818-25.
- 1532 Miller GA (1991) The science of words. Scientific American Library New York:276 pp.
- 1533 Mitchell P (1961) Coupling of phosphorylation to electron and hydrogen transfer by a chemi-osmotic type of
 1534 mechanism. *Nature* 191:144-8.
- 1535 Mitchell P (2011) Chemiosmotic coupling in oxidative and photosynthetic phosphorylation. *Biochim Biophys*
 1536 *Acta Bioenergetics* 1807:1507-38.
- 1537 Mogensen M, Sahlin K, Fernström M, Glinborg D, Vind BF, Beck-Nielsen H, Højlund K (2007) Mitochondrial
 1538 respiration is decreased in skeletal muscle of patients with type 2 diabetes. *Diabetes* 56:1592-9.
- 1539 Mohr PJ, Phillips WD (2015) Dimensionless units in the SI. *Metrologia* 52:40-7.
- 1540 Moreno M, Giacco A, Di Munno C, Goglia F (2017) Direct and rapid effects of 3,5-diiodo-L-thyronine (T2).
 1541 *Mol Cell Endocrinol* 7207:30092-8.
- 1542 Morrow RM, Picard M, Derbeneva O, Leipzig J, McManus MJ, Gouspillou G, Barbat-Artigas S, Dos Santos C,
 1543 Hepple RT, Murdock DG, Wallace DC (2017) Mitochondrial energy deficiency leads to hyperproliferation of
 1544 skeletal muscle mitochondria and enhanced insulin sensitivity. *Proc Natl Acad Sci U S A* 114:2705-10.
- 1545 Murley A, Nunnari J (2016) The emerging network of mitochondria-organelle contacts. *Mol Cell* 61:648-53.

- 1546 National Academies of Sciences, Engineering, and Medicine (2018) International coordination for science data
 1547 infrastructure: Proceedings of a workshop—in brief. Washington, DC: The National Academies Press. doi:
 1548 <https://doi.org/10.17226/25015>.
- 1549 Paradies G, Paradies V, De Benedictis V, Ruggiero FM, Petrosillo G (2014) Functional role of cardiolipin in
 1550 mitochondrial bioenergetics. *Biochim Biophys Acta* 1837:408-17.
- 1551 Pesta D, Gnaiger E (2012) High-Resolution Respirometry. OXPHOS protocols for human cells and
 1552 permeabilized fibres from small biopsies of human muscle. *Methods Mol Biol* 810:25-58.
- 1553 Pesta D, Hoppel F, Macek C, Messner H, Faulhaber M, Kobel C, Parson W, Burtcher M, Schocke M, Gnaiger
 1554 E (2011) Similar qualitative and quantitative changes of mitochondrial respiration following strength and
 1555 endurance training in normoxia and hypoxia in sedentary humans. *Am J Physiol Regul Integr Comp Physiol*
 1556 301:R1078–87.
- 1557 Price TM, Dai Q (2015) The role of a mitochondrial progesterone receptor (PR-M) in progesterone action.
 1558 *Semin Reprod Med* 33:185-94.
- 1559 Puchowicz MA, Varnes ME, Cohen BH, Friedman NR, Kerr DS, Hoppel CL (2004) Oxidative phosphorylation
 1560 analysis: assessing the integrated functional activity of human skeletal muscle mitochondria – case studies.
 1561 *Mitochondrion* 4:377-85. Puntschart A, Claassen H, Jostardt K, Hoppeler H, Billeter R (1995) mRNAs of
 1562 enzymes involved in energy metabolism and mtDNA are increased in endurance-trained athletes. *Am J*
 1563 *Physiol* 269:C619-25.
- 1564 Quiros PM, Mottis A, Auwerx J (2016) Mitonuclear communication in homeostasis and stress. *Nat Rev Mol*
 1565 *Cell Biol* 17:213-26.
- 1566 Rackham O, Mercer TR, Filipovska A (2012) The human mitochondrial transcriptome and the RNA-binding
 1567 proteins that regulate its expression. *WIREs RNA* 3:675–95.
- 1568 Reichmann H, Hoppeler H, Mathieu-Costello O, von Bergen F, Pette D (1985) Biochemical and ultrastructural
 1569 changes of skeletal muscle mitochondria after chronic electrical stimulation in rabbits. *Pflugers Arch* 404:1-
 1570 9.
- 1571 Renner K, Amberger A, Konwalinka G, Gnaiger E (2003) Changes of mitochondrial respiration, mitochondrial
 1572 content and cell size after induction of apoptosis in leukemia cells. *Biochim Biophys Acta* 1642:115-23.
- 1573 Rich P (2003) Chemiosmotic coupling: The cost of living. *Nature* 421:583.
- 1574 Rostovtseva TK, Sheldon KL, Hassanzadeh E, Monge C, Saks V, Bezrukov SM, Sackett DL (2008) Tubulin
 1575 binding blocks mitochondrial voltage-dependent anion channel and regulates respiration. *Proc Natl Acad Sci*
 1576 *USA* 105:18746-51.
- 1577 Rustin P, Parfait B, Chretien D, Bourgeron T, Djouadi F, Bastin J, Rötig A, Munnich A (1996) Fluxes of
 1578 nicotinamide adenine dinucleotides through mitochondrial membranes in human cultured cells. *J Biol Chem*
 1579 271:14785-90.
- 1580 Saks VA, Veksler VI, Kuznetsov AV, Kay L, Sikk P, Tiivel T, Tranqui L, Olivares J, Winkler K, Wiedemann F,
 1581 Kunz WS (1998) Permeabilised cell and skinned fiber techniques in studies of mitochondrial function in
 1582 vivo. *Mol Cell Biochem* 184:81-100.
- 1583 Salabei JK, Gibb AA, Hill BG (2014) Comprehensive measurement of respiratory activity in permeabilized cells
 1584 using extracellular flux analysis. *Nat Protoc* 9:421-38.
- 1585 Sazanov LA (2015) A giant molecular proton pump: structure and mechanism of respiratory complex I. *Nat Rev*
 1586 *Mol Cell Biol* 16:375-88.
- 1587 Schneider TD (2006) Claude Shannon: biologist. The founder of information theory used biology to formulate
 1588 the channel capacity. *IEEE Eng Med Biol Mag* 25:30-3.
- 1589 Schönfeld P, Dymkowska D, Wojtczak L (2009) Acyl-CoA-induced generation of reactive oxygen species in
 1590 mitochondrial preparations is due to the presence of peroxisomes. *Free Radic Biol Med* 47:503-9.
- 1591 Schultz J, Wiesner RJ (2000) Proliferation of mitochondria in chronically stimulated rabbit skeletal muscle--
 1592 transcription of mitochondrial genes and copy number of mitochondrial DNA. *J Bioenerg Biomembr* 32:627-
 1593 34.
- 1594 Spejjer D (2016) Being right on Q: shaping eukaryotic evolution. *Biochem J* 473:4103-27.
- 1595 Sugiura A, Mattie S, Prudent J, McBride HM (2017) Newly born peroxisomes are a hybrid of mitochondrial and
 1596 ER-derived pre-peroxisomes. *Nature* 542:251-4.
- 1597 Simson P, Jepihhina N, Laasmaa M, Peterson P, Birkedal R, Vendelin M (2016) Restricted ADP movement in
 1598 cardiomyocytes: Cytosolic diffusion obstacles are complemented with a small number of open mitochondrial
 1599 voltage-dependent anion channels. *J Mol Cell Cardiol* 97:197-203.
- 1600 Stucki JW, Ineichen EA (1974) Energy dissipation by calcium recycling and the efficiency of calcium transport
 1601 in rat-liver mitochondria. *Eur J Biochem* 48:365-75.
- 1602 Tonkonogi M, Harris B, Sahlin K (1997) Increased activity of citrate synthase in human skeletal muscle after a
 1603 single bout of prolonged exercise. *Acta Physiol Scand* 161:435-6.
- 1604 Vamecq J, Schepers L, Parmentier G, Mannaerts GP (1987) Inhibition of peroxisomal fatty acyl-CoA oxidase by
 1605 antimycin A. *Biochem J* 248:603-7.

- 1606 Waczulikova I, Habodaszova D, Cagalinec M, Ferko M, Ulicna O, Mateasik A, Sikurova L, Ziegelhöffer A
1607 (2007) Mitochondrial membrane fluidity, potential, and calcium transients in the myocardium from acute
1608 diabetic rats. *Can J Physiol Pharmacol* 85:372-81.
- 1609 Wagner BA, Venkataraman S, Buettner GR (2011) The rate of oxygen utilization by cells. *Free Radic Biol Med*
1610 51:700-712.
- 1611 Wang H, Hiatt WR, Barstow TJ, Brass EP (1999) Relationships between muscle mitochondrial DNA content,
1612 mitochondrial enzyme activity and oxidative capacity in man: alterations with disease. *Eur J Appl Physiol*
1613 *Occup Physiol* 80:22-7.
- 1614 Watt IN, Montgomery MG, Runswick MJ, Leslie AG, Walker JE (2010) Bioenergetic cost of making an
1615 adenosine triphosphate molecule in animal mitochondria. *Proc Natl Acad Sci U S A* 107:16823-7.
- 1616 Weibel ER, Hoppeler H (2005) Exercise-induced maximal metabolic rate scales with muscle aerobic capacity. *J*
1617 *Exp Biol* 208:1635-44.
- 1618 White DJ, Wolff JN, Pierson M, Gemmell NJ (2008) Revealing the hidden complexities of mtDNA inheritance.
1619 *Mol Ecol* 17:4925-42.
- 1620 Wikström M, Hummer G (2012) Stoichiometry of proton translocation by respiratory complex I and its
1621 mechanistic implications. *Proc Natl Acad Sci U S A* 109:4431-6.
- 1622 Willis WT, Jackman MR, Messer JI, Kuzmiak-Glancy S, Glancy B (2016) A simple hydraulic analog model of
1623 oxidative phosphorylation. *Med Sci Sports Exerc* 48:990-1000.